



CERN-EP-2025-221
LHCb-PAPER-2025-036
October 16, 2025

Measurement of CP asymmetry in $D^0 \rightarrow K_S^0 K_S^0$ decays with the LHCb Upgrade I detector

LHCb collaboration[†]

Abstract

A measurement of CP asymmetry in $D^0 \rightarrow K_S^0 K_S^0$ decays is reported, based on a data sample of proton-proton collisions collected with the LHCb Upgrade I detector in 2024 at a centre-of-mass energy of 13.6 TeV, corresponding to an integrated luminosity of 6.2 fb^{-1} . The $D^0 \rightarrow K_S^0 \pi^+ \pi^-$ decay is used as calibration channel to cancel residual detection and production asymmetries. The time-integrated CP asymmetry for the $D^0 \rightarrow K_S^0 K_S^0$ mode is measured to be

$$\mathcal{A}^{CP}(D^0 \rightarrow K_S^0 K_S^0) = (1.86 \pm 1.04 \pm 0.41)\%,$$

where the first uncertainty is statistical, and the second is systematic. This is the most precise determination of this quantity to date.

Submitted to JHEP

© 2025 CERN for the benefit of the LHCb collaboration. [CC BY 4.0 licence](#).

[†]Authors are listed at the end of this paper.

1 Introduction

Violation of charge-parity (CP) symmetry in charm-quark transitions has been observed for the first time in the measurement of the difference between the CP asymmetry in $D^0 \rightarrow K^+K^-$ and $D^0 \rightarrow \pi^+\pi^-$ decays [1]. As of today, this measurement remains the only experimental evidence of CP violation in charm decays, and more generally in any up-type quark (u , c , or t) transition. A successive measurement in the $D^0 \rightarrow K^+K^-$ decay mode found no statistically significant CP asymmetry [2], leaving the $D^0 \rightarrow \pi^+\pi^-$ decay as the only charm-hadron decay with experimental evidence of CP violation [3, 4].

While the existence of CP violation in the charm-quark sector at the observed $\mathcal{O}(10^{-3})$ level is not excluded in the Standard Model (SM), uncertainties in theoretical calculations do not allow for a quantitative comparison or precise predictions for other decay channels [5–16]; see Refs. [17–19] for reviews on this subject. Further experimental measurements of CP asymmetries in charm decays are therefore highly desirable, as they would provide deeper insight into CP violation phenomenology. Such measurements could potentially involve dynamics beyond the SM [20–26], that are not constrained to be the same as in the down-type quark (d , s , or b) sector.

Among many charm-hadron decay modes in which CP violation could manifest itself, the Cabibbo-suppressed $D^0 \rightarrow K_S^0 K_S^0$ mode stands out for being analogous to the two-body decays $D^0 \rightarrow K^+K^-$ and $D^0 \rightarrow \pi^+\pi^-$ [1], but has the possibility of a more sizeable asymmetry. Only amplitudes proceeding via tree-level exchange – which vanish in the flavour-SU(3) limit – and electroweak loop diagrams contribute to this decay, which therefore has a relatively small branching fraction [27]. Its CP asymmetry is defined by

$$\mathcal{A}^{CP}(K_S^0 K_S^0) \equiv \frac{\Gamma(D^0 \rightarrow K_S^0 K_S^0) - \Gamma(\bar{D}^0 \rightarrow K_S^0 K_S^0)}{\Gamma(D^0 \rightarrow K_S^0 K_S^0) + \Gamma(\bar{D}^0 \rightarrow K_S^0 K_S^0)}, \quad (1)$$

with Γ being the decay width of the neutral D meson. Any effect arising from regeneration, mixing and CP violation in the $K_S^0 K_S^0$ final state cancel in \mathcal{A}^{CP} , since the D^0 and \bar{D}^0 decay to the same CP -symmetric $K^0 - \bar{K}^0$ final state [28]. In the SM, $\mathcal{A}^{CP}(K_S^0 K_S^0)$ might be significantly larger than in the $D^0 \rightarrow \pi^+\pi^-$ and $D^0 \rightarrow K^+K^-$ channels. Several predictions exist for $\mathcal{A}^{CP}(K_S^0 K_S^0)$ [9, 29–32], up to the percent level. The study of the $D^0 \rightarrow K_S^0 K_S^0$ decay mode provides a valuable probe of CP violation in the charm sector, offering a means to discriminate between competing theoretical approaches.

These considerations have motivated several experimental determinations of this observable across different experiments, including some recent ones [33–38]. The world average of the CP asymmetry is $\mathcal{A}^{CP}(K_S^0 K_S^0) = (-1.19 \pm 0.77 \pm 0.17)\%$, where the time-dependent contribution to the asymmetry is neglected [39, 40]. This has now reached the subpercent level, entering the interesting sensitivity range of theoretical predictions. The reduced precision of this measurement compared with other charm CP asymmetry results is due to the smaller branching fraction and the difficulty of reconstructing the K_S^0 decay products, given its much longer lifetime relative to bottom and charm hadrons.

In this work, a new measurement of $\mathcal{A}^{CP}(K_S^0 K_S^0)$ is reported, based on a sample of proton-proton (pp) collisions corresponding to an integrated luminosity of about 6.2 fb^{-1} , collected in 2024 by the LHCb Upgrade I detector. The detector has been significantly improved over its previous version, including the data acquisition system [41, 42], which enabled the adoption of a software-based selection of K_S^0 particles at the first trigger level, resulting in a substantially improved efficiency.

The measurement of $\mathcal{A}^{CP}(K_S^0 K_S^0)$ requires knowledge of the D^0 flavour at production. A sample of flavour-tagged $D^0 \rightarrow K_S^0 K_S^0$ decays is obtained by selecting only D^0 mesons that originate from $D^*(2010)^+ \rightarrow D^0 \pi^+$ decays.¹ The charge of the pion in this decay (“tagging pion”) identifies the flavour of the accompanying neutral charm meson. While $D^0 - \bar{D}^0$ oscillations can cause a flavour change before decay, the effect is small compared with the resolution of the current measurement and is therefore neglected [43]. The K_S^0 mesons are reconstructed in the $\pi^+ \pi^-$ final state.

The decay widths Γ in Eq. 1 are related to the observed yields N by

$$N(\overline{D}^0 \rightarrow K_S^0 K_S^0) \propto \varepsilon^\pm(D^{*\pm}) \sigma(D^{*\pm}) \Gamma(\overline{D}^0 \rightarrow K_S^0 K_S^0), \quad (2)$$

where $\sigma(D^{*\pm})$ denotes the production cross-sections of the $D^{*\pm}$ mesons and $\varepsilon^\pm(D^{*\pm})$ the corresponding detection efficiencies for their decays. Both factors are charge asymmetric, due to the $D^{*\pm}$ production asymmetry arising from the hadronisation of charm quarks in pp collisions, and to asymmetries in the geometry and response of the detector. Since the final state of the D^0 decay is self-conjugate, any detection asymmetry arises solely from the tagging pion. All these quantities are calibrated using a sample of $D^0 \rightarrow K_S^0 \pi^+ \pi^-$ decays, which have the same final-state particles as the $D^0 \rightarrow K_S^0 K_S^0$ decay, but with a negligible CP asymmetry [18]. In order to avoid experimenter’s bias, the results of the analysis were not examined until the full procedure had been finalised.

2 LHCb detector

The LHCb Upgrade I detector [44] is a single-arm forward spectrometer covering the pseudorapidity range $2 < \eta < 5$, designed for the study of particles containing b or c quarks. The detector was installed prior to the Run 3 data-taking period, which started in 2022. The LHCb Upgrade I detector represents a major change of the detector system and was designed to match the performance of the Run 1–2 detector [44, 45], while allowing it to operate at approximately five times the luminosity.

The high-precision tracking system consists of a silicon-pixel vertex detector (VELO) surrounding the pp interaction region [46], a large-area silicon-strip detector (UT) [47] located upstream of a dipole magnet with a bending power of about 4 T m, and three stations of scintillating-fibre detectors [47] located downstream of the magnet. Tracks reconstructed in both the VELO and the scintillating-fiber detectors, with the possible addition of intermediate hits in UT, are referred to as *long* tracks. The dipole magnetic-field polarity is periodically reversed during data taking, alternating between pointing upwards (*MagUp*) and downwards (*MagDown*), to mitigate the effects of differences in reconstruction efficiencies for particles of opposite charges. Different types of charged hadrons are distinguished using information from two ring-imaging Cherenkov detectors [48].

Readout of all detectors into an all-software trigger [41, 42] is a central feature of the upgraded detector, allowing the reconstruction of events at the maximum LHC interaction rate, and their selection in real time. The trigger system is implemented in two stages: a first inclusive stage (HLT1) running on GPU boards based primarily on charged particle reconstruction, which reduces the data volume by roughly a factor of twenty, and a second

¹Inclusion of the charge-conjugate process is implied throughout this document unless explicitly specified. Hereafter, the $D^*(2010)^+$ meson is referred to as D^{*+} .

stage (HLT2) running on CPUs, which performs the full offline-quality reconstruction and selection of physics signatures. A large disk buffer is placed between these stages to hold the data while the real-time alignment and calibration are performed.

For the measurement described in this paper, data collection benefits from the newly implemented trigger system, which, for the first time, enables the selection of events containing K_S^0 candidates directly at the HLT1 level for every LHC bunch crossing. This leads to an improvement in the signal efficiency by a factor of about three over the previous LHCb detector, which is the main factor responsible for the increase in precision for the current measurement.

Simulated samples are used solely to optimise selection requirements. In the simulation, pp collisions are generated using PYTHIA [49] with a specific LHCb configuration [50]. Decays of unstable particles are described by EVTGEN [51], in which final-state radiation is generated using PHOTOS [52]. The interaction of the generated particles with the detector, and its response, are implemented using the GEANT4 toolkit [53] as described in Ref. [54].

3 Event selection

At the HLT1 stage, long tracks with good fit χ^2 , momentum $p > 5 \text{ GeV}/c$, transverse momentum $p_T > 0.45 \text{ GeV}/c$, and incompatible with originating from any reconstructed primary vertex (PV) are considered. The tracks with opposite charge passing this selection are paired, and their invariant mass is computed assuming the pion mass for each of them. Pairs with an invariant mass within $\pm 45 \text{ MeV}/c^2$ of the known K_S^0 mass [27] are classified as K_S^0 candidates. Events of interest for this analysis are triggered by requiring at least one K_S^0 candidate with $p_T > 2.45 \text{ GeV}/c$.

At the HLT2 level, after a full reconstruction of the whole event, K_S^0 candidates with an invariant mass within $\pm 35 \text{ MeV}/c^2$ from the known K_S^0 mass are paired to form D^0 candidates. These candidates are required to originate from a common vertex and to have an invariant mass within $\pm 90 \text{ MeV}/c^2$ of the known D^0 mass [27]. An additional track is then combined with the D^0 particle to form D^{*+} candidates. The invariant-mass difference $\Delta m = m(D^{*+}) - m(D^0)$ is required to be smaller than $170 \text{ MeV}/c^2$ [27]. The resulting candidates are saved on permanent storage and used for further analysis.

A calibration sample of $D^{*+} \rightarrow D^0(K_S^0\pi^+\pi^-)\pi^+$ decays is obtained from the same HLT1 trigger selection, by applying a similar HLT2 selection, in which the requirements on the second K_S^0 of the signal mode are replaced by requirements on the compatibility of the two pions to have originated from the D^0 decay vertex. This HLT2 selection is specifically developed for the purpose of the current work, with the aim of providing a calibration sample with the closest trigger selections to that of the signal decay. Events collected via other parallel trigger selections are not considered. This ensures an accurate cancellation of detector effects between samples across all periods of data taking, notwithstanding the changes in detector and trigger conditions made over time to optimize the global apparatus performance.

The offline selection of candidate decays is designed to suppress the background while avoiding introducing any charge biases that might affect the signal and calibration mode differently. In this respect, an important aspect is the presence, in both the signal and calibration sample, of a non-negligible fraction of charm mesons originating from b -hadron

decays rather than from the primary pp interaction. These secondary particles are affected by different production asymmetries with respect to the prompt decays, quantified at the 0.2% level [55]. Following the same approach as the previous LHCb measurement [35], it has not been attempted to reject secondary decays, but rather allow them to contribute to the measurement. The spurious asymmetry introduced by the secondary component is cancelled by ensuring that the calibration sample contains secondary decays in the same proportion as the signal sample. This is achieved by a careful choice of the selection criteria, avoiding imposing any requirements on observables sensitive to the position of the D^{*+} or D^0 vertices that have different resolutions in the two samples [56].

The calibration mode has the same final-state particles as the signal, and a branching fraction approximately two hundred times larger [27]. This decay mode can contaminate the signal even though the proportion of pion pairs randomly falling within the K_S^0 mass window is small. Although the fit procedure is capable of taking this contribution into account, additional selection criteria are applied on the significance of the flight distance of both K_S^0 mesons from the D^0 decay vertex to suppress this contamination to a negligible level. The effect of this requirement is independent of the flight distance of the parent charm meson from the primary pp interaction vertex, and therefore does not affect the proportion of the secondary component. Studies based on simulated events have identified other physics processes that could potentially contaminate the signal sample, such as partially reconstructed D^0 decays originating from D^{*+} meson, including $D^0 \rightarrow K_S^0 K_S^0 \pi^0$ decays. Some non- D^0 decays can also contaminate the sample, with the main contributor being the $D_s^+ \rightarrow K_S^0 K_S^0 \pi^+$ mode, where the $K_S^0 K_S^0$ pair is incorrectly associated with a D^0 decay. These background components are rendered negligible by selecting only candidates with $m(D^0)$ within ± 26 MeV/ c^2 of the known D^0 mass [27], which is measured with a resolution of about 7 MeV/ c^2 . The width of the mass window is chosen to prevent a possible risk of charge biases arising from residual differences in the mass calibration and resolution between positive and negative particles. The potential contamination of the K_S^0 sample by Λ particles has been verified on data, and found to have a negligible impact, since this background does not peak in the Δm distribution.

To maximise the sensitivity of the measurement, only D^{*+} candidates compatible with having decayed in the vicinity of the PV are selected. This suppresses background from random combination of tracks and allows the candidate mass to be recalculated by constraining the origin vertex to coincide with the PV, improving the Δm mass resolution by a factor of two, with an associated improvement in combinatorial background rejection. Using simulated samples it is shown that this requirement removes the same proportion of secondary B -decay component from both the signal and calibration sample, thus leaving the validity of the cancellation procedure unaffected.

The largest remaining background contribution to the signal sample originates from random combinations of genuine K_S^0 particles from the primary interaction, which form a fake D^0 candidate. This is partially rejected by the $m(D^0)$ requirement, and is further suppressed by requiring the K_S^0 candidates to be inconsistent with originating from the PV with a selection on its impact parameter significance, thereby improving the signal purity. To ensure an identical effect on the secondary fraction in signal and calibration samples, the selection is applied only on the K_S^0 candidate that fulfils the HLT1 selection. If both K_S^0 candidates do, one is arbitrarily chosen. A threshold for this requirement has been optimised jointly with a condition on a multivariate classifier. Track-related observables, including track and vertex quality, transverse momenta of K_S^0 and D^0 candidates, helicity

Table 1: Integrated luminosity of individual data blocks.

| Data block | $\int \mathcal{L} dt [fb^{-1}]$ | Polarity |
|------------|---------------------------------|----------------|
| A | 0.7 | <i>MagDown</i> |
| B | 0.7 | <i>MagUp</i> |
| C | 0.6 | <i>MagUp</i> |
| D | 1.1 | <i>MagUp</i> |
| E | 1.1 | <i>MagUp</i> |
| F | 0.9 | <i>MagDown</i> |
| G | 0.7 | <i>MagDown</i> |
| H | 0.4 | <i>MagUp</i> |
| Total | 6.2 | — |

angles of the K_S^0 and D^0 decays, and particle-identification information of the D^0 final-state particles, are used as input to a k -nearest-neighbours (kNN) classifier [57]. This classifier is trained using a simulated $D^0 \rightarrow K_S^0 K_S^0$ sample as signal proxy and data from the D^0 mass sidebands as combinatorial background proxy. Kinematic variables of the tagging pion are excluded from the classifier to avoid introducing possible charge-asymmetry biases.

To make better use of the available data, signal candidates are classified into two classes of purity (high-purity, with signal-to-background ratio $S/B \sim 20$ and low-purity, with $S/B \sim 4$), which are fitted separately to determine \mathcal{A}^{CP} . These classes are defined by an optimised set of requirements on both the kNN classifier and the significance of the K_S^0 impact parameter, chosen to maximise the combined resolution on the \mathcal{A}^{CP} parameter.

This strategy closely follows the procedure of the previous LHCb publication [35]. In about 10% of events, multiple D^{*+} candidates are found. In these cases, only one D^{*+} candidate is arbitrarily selected for subsequent analysis.

The data sample is divided into eight blocks according to data-taking periods with substantially different trigger and detector spatial alignment conditions. These conditions were varied several times during the year to optimise the running of the LHCb Upgrade I detector. The offline selection is the same in each block, except for the requirement on the D^0 mass window, whose threshold has been determined separately for each block to account for possible slight calibration differences. The integrated luminosities of each data block are reported in Table 1.

4 Correction of nuisance asymmetries

Each $D^0 \rightarrow K_S^0 K_S^0$ candidate is appropriately weighted to cancel all spurious production and detection asymmetries, with weights obtained from the calibration sample. This follows the same procedure as the previous LHCb analysis [35], with the only modification that the weights, w^\pm , are expressed in terms of the three-momentum \vec{p} of the tagging pion from the D^{*+} decay instead of using the D^0 kinematic observables

$$w^\pm(\vec{p}) = \frac{n_C^+(\vec{p}) + n_C^-(\vec{p})}{2n_C^\pm(\vec{p})}. \quad (3)$$

This is motivated by the need to precisely control the most important source of detection asymmetry. In Eq. 3, the probability density of calibration decays in the \vec{p} space is denoted by $n_C^\pm(\vec{p})$. The plus and minus signs in the expression indicate quantities related to D^{*+} and D^{*-} candidates, respectively. The weights are computed by classifying the calibration sample based on the observed charge asymmetry by means of a kNN classifier based on the three-dimensional \vec{p} space. The number of neighbours used is 30, as it is low enough to describe local variations of asymmetry across the phase space, and it allows to keep statistical fluctuations related to the size of the considered sample below 10%.

In the calibration sample, the absence of selection criteria requiring compatibility of the D^0 final-state particles with the primary vertex in the dedicated HLT2 selection leads to a low-purity sample. To improve the S/B ratio, additional offline selections are applied, while maintaining strict consistency between the calibration and signal selections to ensure an accurate cancellation of detector effects.

First, all offline selections applied to the signal sample that can be directly ported to the calibration sample are applied to equalise the kinematic distributions and the fraction of secondary decays. Then, requirements on variables including the particle-identification information of final-state tracks, vertex-fit quality of D^0 , K_S^0 and D^{*+} mesons, and the opening angles between the final-state particles are applied to further suppress the combinatorial background. The resulting sample has a high purity ($S/B \sim 13$) and it is used for the weight calculation. The Δm distribution of calibration candidates is shown in Fig. 1. It is verified that the residual background under the Δm peak does not introduce any bias in the measurement.

The newly adopted calibration mode is not self-conjugate, in contrast to the previously used $D^0 \rightarrow K^+ K^-$ decay [35]. To account for this, the analysis procedure is modified with respect to the earlier LHCb measurement. The decay proceeds primarily through the intermediate $D^0 \rightarrow K^{*-}(K_S^0 \pi^-) \pi^+$ channel, which produces a charge-asymmetric momentum distribution of the two pions. As a result, the detector response may differ between signal and calibration candidates, since positive and negative pions traverse regions with distinct charge-dependent detection asymmetries in the two samples. To eliminate this spurious effect, the three-momentum of the pions from the D^0 decay is weighted in the calibration sample to make it charge symmetric, before being used as input to the kNN classifier that calculates the signal weights. The charge-symmetrisation procedure employs an independent kNN classifier, trained to distinguish candidates based on the charge of the highest-momentum pion and the kinematics of both final-state pions. The effectiveness of this correction is confirmed by verifying that a kNN classifier can no longer separate D^0 from \bar{D}^0 after the weights are applied. The correction shifts the final result by about 0.1%, corresponding to roughly 14% of the statistical uncertainty, and the associated systematic uncertainty is therefore negligible compared to other contributions.

Distributions of the final weights w^\pm applied to the signal sample for the correction of spurious asymmetries (as defined in Eq. 3) are shown in Fig. 2. The differences between the distributions of the two charges are a consequence of different D^0 and \bar{D}^0 acceptances and detector asymmetries. These distributions are similar, but not identical, in every data block, and D^0/\bar{D}^0 candidates are separately corrected before fitting for the asymmetry. To avoid weights affected by large uncertainties, candidates with weights lower than 0.56 and larger than 5.00 are dropped at this stage. These correspond to a fraction of 5×10^{-4} , whose effects are therefore neglected. The size of the asymmetry correction obtained by the application of these weights is about 1.4%. This accounts for the cumulative effect of

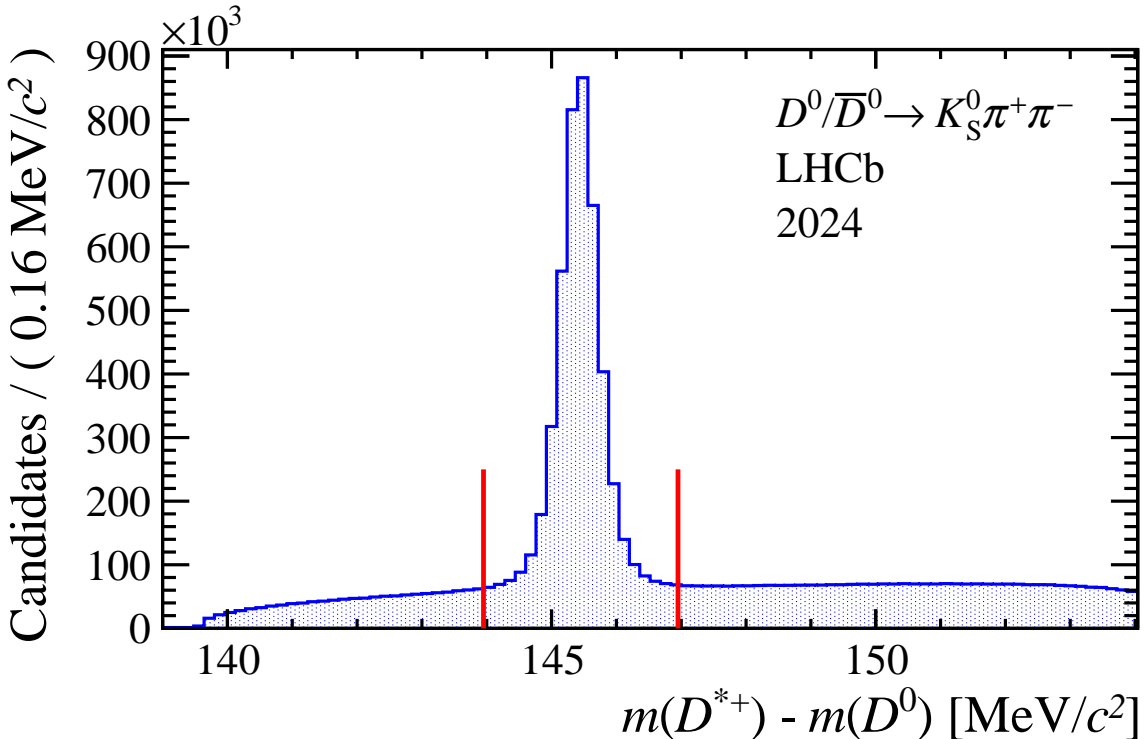


Figure 1: Distribution of $\Delta m = m(D^{*+}) - m(D^0)$ for $D^0 \rightarrow K_S^0 \pi^+ \pi^-$ candidates, after application of all offline selections. Calibration candidates are selected by the requirement $|\Delta m - 145.45 \text{ MeV}/c^2| < 1.5 \text{ MeV}/c^2$, shown in red.

all production and detection asymmetries affecting the data.

5 Asymmetry measurement

A binned maximum-likelihood fit to the joint distribution of Δm and the two $m(K_S^0)$ observables is performed separately for each data block to measure the \mathcal{A}^{CP} parameter. The choice of the K_S^0 candidate for filling the invariant-mass histograms is arbitrary. The three-dimensional fit is performed simultaneously for candidates of both flavours and across the two purity bins. Data block A is further divided into two sections, fitted separately to account for changes in running conditions. The final measurement is then obtained as the weighted average of the results from all blocks.

The total probability density function is parametrised by the sum of the signal component, which has a peaking distribution in each of the three observables, and four background components, each describing a specific source: random combination of five pions, a K_S^0 combined with three random pions, three random pions combined with a K_S^0 , two K_S^0 combined with a random pion. The probability density functions used to describe the five components are empirical. The contributions from $D^0 \rightarrow K_S^0 \pi^+ \pi^-$ and $D^0 \rightarrow \pi^+ \pi^- \pi^+ \pi^-$ decays are verified to be negligible, and are excluded from the fit. The peaking component in the Δm distribution is described by a Johnson S_U distribution [58]. The peaking component in the $m(K_S^0)$ distribution is modelled as the sum of two Gaussian functions with a common mean but different widths, except for blocks A, B, and H, where

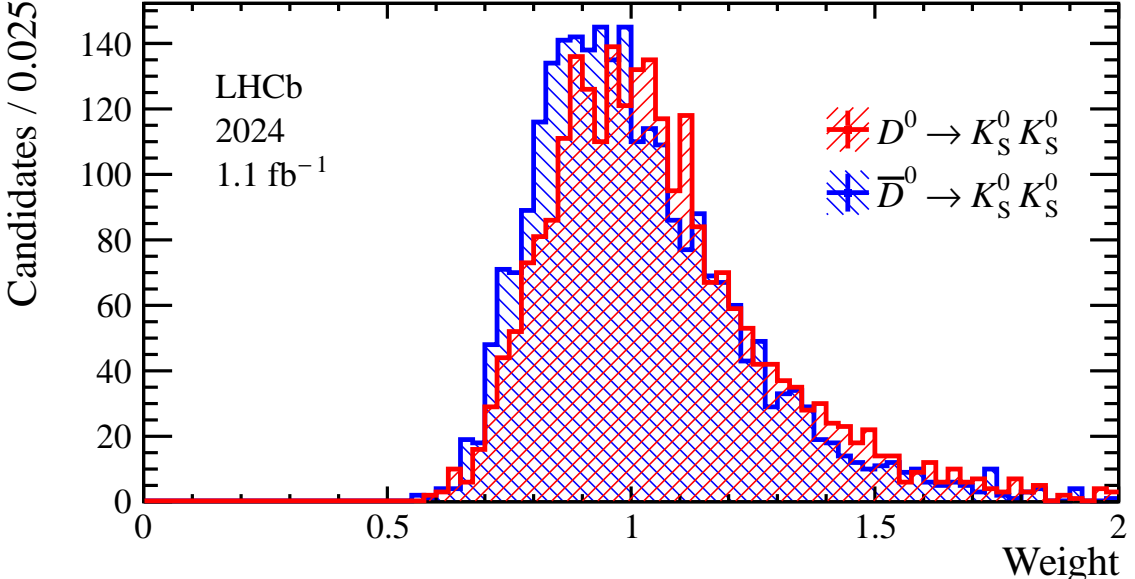


Figure 2: Example (data block D) of distributions of weights applied to signal candidates. These are used in the fit extracting $\mathcal{A}^{CP}(K_S^0 K_S^0)$ to correct the signal sample for detection and production asymmetries of the calibration channel.

a single Gaussian function is used to avoid fit instabilities due to their smaller sample sizes. The nonpeaking component in the Δm distribution is modelled with a threshold function in the low-purity bins and with a first-order polynomial in the high-purity bins. In the $m(K_S^0)$ distribution, this component is described by a first-order polynomial.

In each subsample, the parameters defining the signal and background probability density functions are shared between D^{*+}/D^{*-} candidates, while the normalisation of each component is allowed to differ. All parameters included in the probability density function are allowed to vary in the fit to the data.

Figures 3 and 4 show the projections of the fit to the total data sample for candidates satisfying the high- and low-purity selection, respectively. The histograms are obtained by adding all data blocks. The candidates entering these plots have been individually weighted to correct for spurious asymmetries.

6 Systematic uncertainties and cross-checks

To assess potential systematic effects, the weighting procedure is validated by applying the weights derived from one half of the calibration sample to the other half. As expected, this cancels the raw asymmetry of the sample, which was initially significant at $(-1.04 \pm 0.05)\%$ due to a combination of production asymmetry and detector effects, and reduces it to $(-0.08 \pm 0.07)\%$ after the application of the weights.

The weighting procedure is also affected by a systematic uncertainty, partly due to the finite size of the calibration sample, and partly due to the numerical approximation, which is implicit in estimating a ratio of probability densities with the discretised kNN classifier output. The first uncertainty is evaluated by a bootstrap procedure applied to the calibration sample, where multiple pseudoexperiments are generated by resampling.

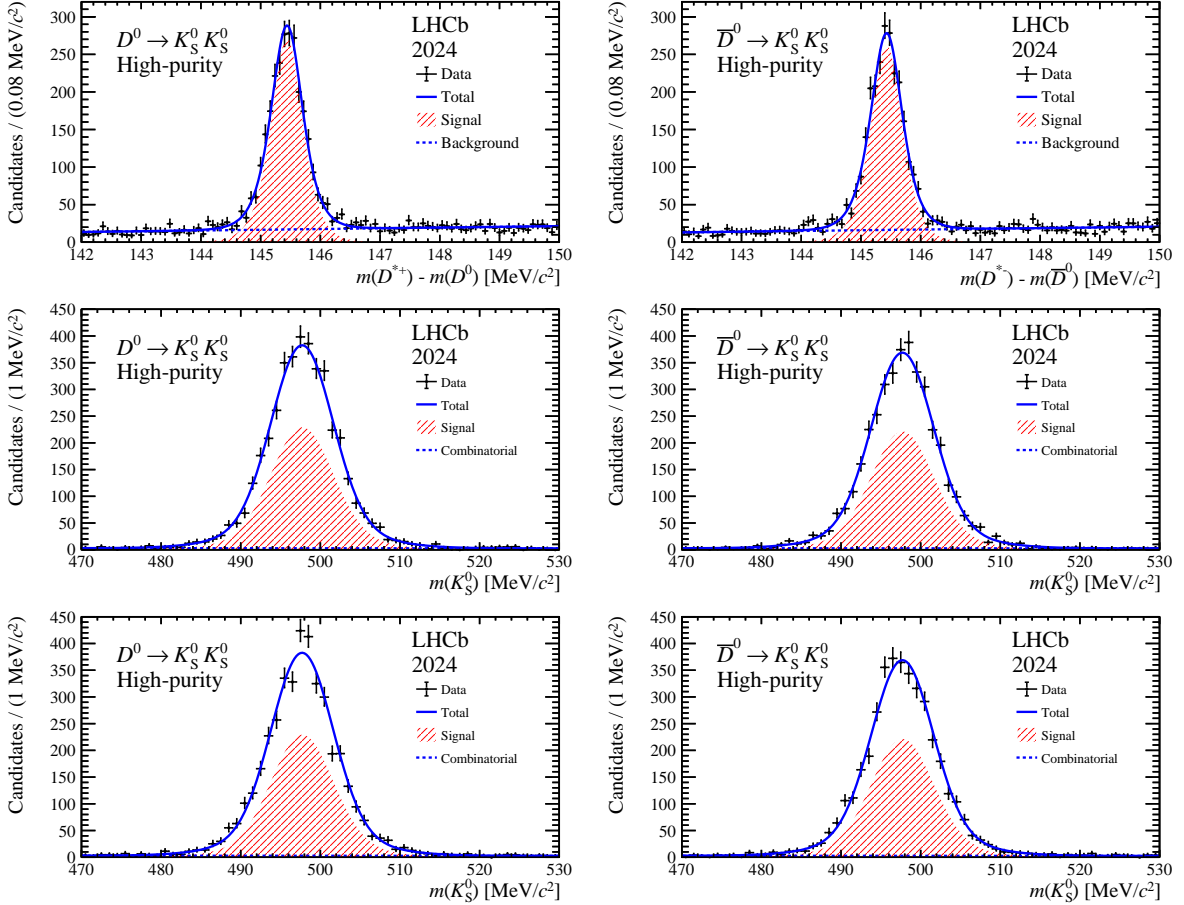


Figure 3: Results of the fit for the sample satisfying the high-purity selection and combining all data blocks. The left (right) column reports histograms for the D^0 (\bar{D}^0) candidates. The Δm distributions are reported in the top row. The masses of the two K_S^0 candidates are reported in the middle and bottom rows. The $D^0 \rightarrow K_S^0 K_S^0$ component is indicated by the red area. For the $m(K_S^0)$ distributions the combinatorial component refers to random combination of pions.

The resulting uncertainty is 0.24%. The second effect is evaluated by varying the value of the number of neighbours (k parameter) used in the kNN classifier when computing the weights, considering values between 30 and 200. This yields an uncertainty of 0.20%.

While asymmetries arising from regeneration and from mixing and CP violation in the $K^0 - \bar{K}^0$ system do not affect the signal sample, they can affect the $D^0 \rightarrow K_S^0 \pi^+ \pi^-$ calibration sample. To evaluate the impact of the neglected K_S^0 regeneration and oscillation, the dependence of \mathcal{A}^{CP} (after applying all weights) on the K_S^0 flight distance is studied using the calibration data. No evidence of such a dependence is observed, and an upper limit of 0.05% is set on the corresponding \mathcal{A}^{CP} bias, which is negligible compared to the statistical and other systematic uncertainties.

An additional source of systematic uncertainty arises from the limited knowledge of the shape of the mass distributions. It is evaluated by fitting the simulated samples of pseudoexperiments with alternative models, whose fit quality is comparable to that of the baseline model. The alternative models include: the sum of two Gaussian functions for the peaking component in the Δm distribution; the sum of three Gaussian functions for the peaking component in the $m(K_S^0)$ distribution; and a polynomial multiplied by a threshold

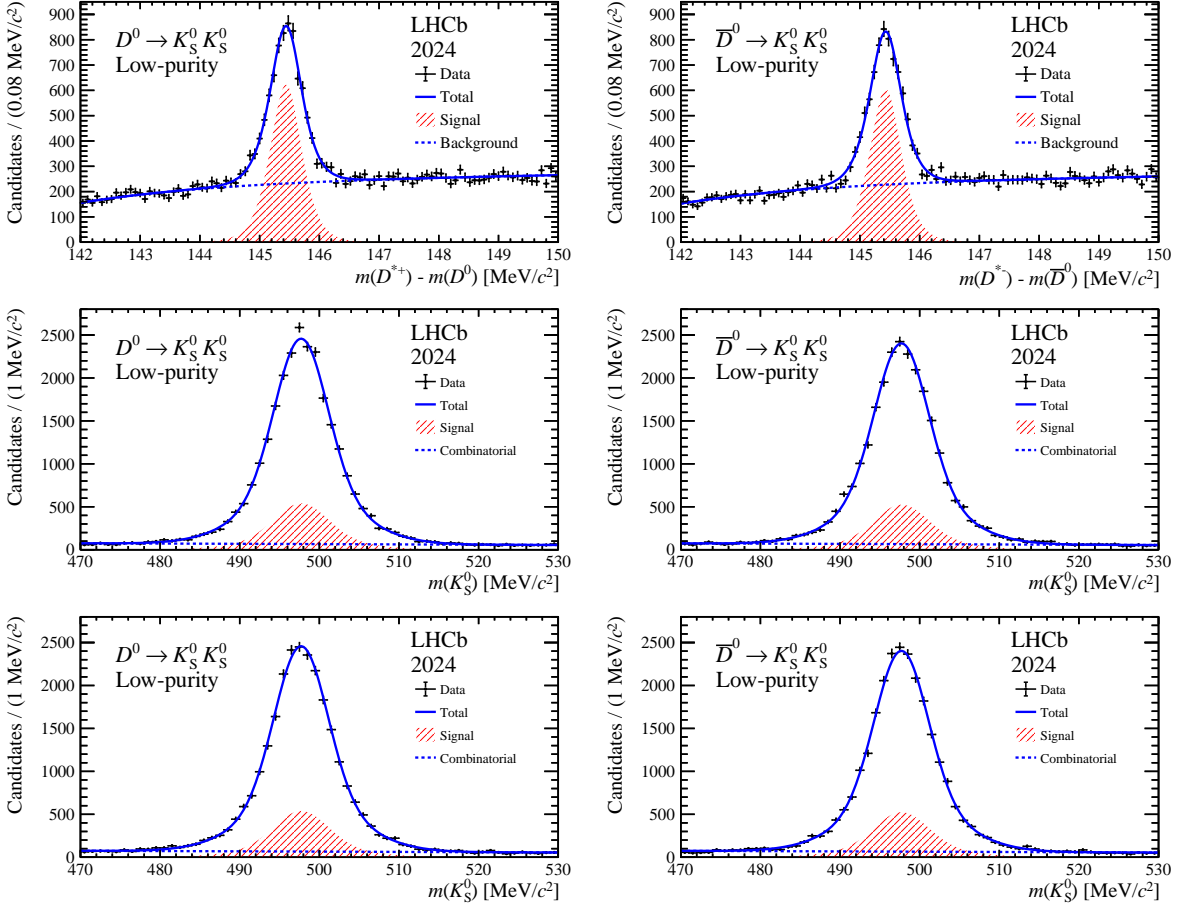


Figure 4: Results of the fit for the sample satisfying the low purity selection and integrating all data blocks. The left (right) column reports histograms for the D^0 (\bar{D}^0) candidates. The Δm distributions are reported in the top row. The masses of the two K_S^0 candidates are reported in the middle and bottom rows. The $D^0 \rightarrow K_S^0 K_S^0$ component is indicated by the red area. For the $m(K_S^0)$ distributions the combinatorial component refers to random combination of pions.

Table 2: Summary of absolute systematic uncertainty sources on $\mathcal{A}^{CP}(D^0 \rightarrow K_S^0 K_S^0)$ in percent.

| Systematic source | Uncertainty [%] |
|-------------------------|-----------------|
| Calibration sample size | 0.24 |
| Weighting procedure | 0.20 |
| Fit model | 0.27 |

function for the nonpeaking component in the Δm distribution. The largest observed variations are taken as the systematic uncertainty ranging from 0.1% to 1.9%, depending on the subsample. The systematic uncertainties due to the choice of fit model are assumed to be fully correlated across the data blocks, resulting in a total systematic uncertainty associated with the choice of the fit model of 0.27%. A summary of all systematic effects can be found in Table 2.

The data sample includes data blocks recorded with each polarity of the LHCb magnet. To check for potential uncompensated systematic effects, the asymmetries of the signal and calibration mode have been compared separately for the *MagUp* and *MagDown* magnet

Table 3: Measurements of yields and $\mathcal{A}^{CP}(D^0 \rightarrow K_S^0 K_S^0)$ extracted from weighted fits to individual data blocks. The quoted uncertainty is statistical only.

| Data block | Yield | \mathcal{A}^{CP} [%] |
|------------|---------------|------------------------|
| A | 1534 ± 75 | 5.5 ± 3.4 |
| B | 1639 ± 56 | 0.8 ± 3.2 |
| C | 1385 ± 55 | -0.3 ± 3.4 |
| D | 2915 ± 85 | 0.3 ± 2.4 |
| E | 3149 ± 94 | 0.0 ± 2.4 |
| F | 2544 ± 77 | 4.6 ± 2.6 |
| G | 1599 ± 67 | 1.7 ± 3.3 |
| H | 911 ± 54 | 5.6 ± 4.3 |

polarities. The results are found to be compatible within 1.5σ .

7 Results

The measured $\mathcal{A}^{CP}(D^0 \rightarrow K_S^0 K_S^0)$ values for the different data blocks are shown in Table 3. All measurements are compatible with each other. The weighted average is

$$\mathcal{A}^{CP}(K_S^0 K_S^0) = (1.86 \pm 1.04 \pm 0.41)\%,$$

where the first uncertainty is statistical, and the second is systematic, obtained by combining the individual sources of systematic uncertainty from Table 2 as uncorrelated. This result is the most precise single measurement of this quantity to date, and it is compatible with CP symmetry and with the average of previous determinations [33–38]. Any time-dependent effect can be neglected, as mentioned in Section 1. It is anyway useful to provide the average decay time of the selected $D^0 \rightarrow K_S^0 K_S^0$ decays to allow the interpretation of this result in a wider global charm CP violation scenario. This value normalised to the D^0 lifetime [27], is $\langle t \rangle / \tau(D^0) = 1.76 \pm 0.02$. It is obtained by integrating all data blocks and purity bins, after performing sideband subtraction in the Δm distribution. The contribution from secondary decays is subtracted, exploiting the same simulated $D^0 \rightarrow K_S^0 K_S^0$ sample used for selections optimization. The quoted uncertainty includes statistical and systematic contributions.

Combining this result with the previous LHCb measurements [34, 35], assuming all systematic uncertainties are uncorrelated, the following value is obtained

$$\mathcal{A}^{CP}(K_S^0 K_S^0) = (-0.37 \pm 0.78 \pm 0.29)\%.$$

The compatibility between the three measurements corresponds to a p-value of 1.2%. Despite the similar integrated luminosity of the LHCb measurement based on the 2015–2018 dataset, and the exclusion of certain candidate categories included in the previous analysis [35], this result achieves better precision, thanks to the significantly improved efficiency of the upgraded trigger.

Acknowledgements

We express our gratitude to our colleagues in the CERN accelerator departments for the excellent performance of the LHC. We thank the technical and administrative staff at the LHCb institutes. We acknowledge support from CERN and from the national agencies: ARC (Australia); CAPES, CNPq, FAPERJ and FINEP (Brazil); MOST and NSFC (China); CNRS/IN2P3 (France); BMFTR, DFG and MPG (Germany); INFN (Italy); NWO (Netherlands); MNiSW and NCN (Poland); MCID/IFA (Romania); MICIU and AEI (Spain); SNSF and SER (Switzerland); NASU (Ukraine); STFC (United Kingdom); DOE NP and NSF (USA). We acknowledge the computing resources that are provided by ARDC (Australia), CBPF (Brazil), CERN, IHEP and LZU (China), IN2P3 (France), KIT and DESY (Germany), INFN (Italy), SURF (Netherlands), Polish WLCG (Poland), IFIN-HH (Romania), PIC (Spain), CSCS (Switzerland), and GridPP (United Kingdom). We are indebted to the communities behind the multiple open-source software packages on which we depend. Individual groups or members have received support from Key Research Program of Frontier Sciences of CAS, CAS PIFI, CAS CCEPP, Fundamental Research Funds for the Central Universities, and Sci. & Tech. Program of Guangzhou (China); Minciencias (Colombia); EPLANET, Marie Skłodowska-Curie Actions, ERC and NextGenerationEU (European Union); A*MIDEX, ANR, IPhU and Labex P2IO, and Région Auvergne-Rhône-Alpes (France); Alexander-von-Humboldt Foundation (Germany); ICSC (Italy); Severo Ochoa and María de Maeztu Units of Excellence, GVA, XuntaGal, GENCAT, InTalent-Inditex and Prog. Atracción Talento CM (Spain); SRC (Sweden); the Leverhulme Trust, the Royal Society and UKRI (United Kingdom).

References

- [1] LHCb collaboration, R. Aaij *et al.*, *Observation of CP violation in charm decays*, Phys. Rev. Lett. **122** (2019) 211803, [arXiv:1903.08726](#).
- [2] LHCb collaboration, R. Aaij *et al.*, *Measurement of the time-integrated CP asymmetry in $D^0 \rightarrow K^- K^+$ decays*, Phys. Rev. Lett. **131** (2023) 091802, [arXiv:2209.03179](#).
- [3] LHCb collaboration, *Simultaneous determination of the CKM angle γ and parameters related to mixing and CP violation in the charm sector*, LHCb-CONF-2024-004, 2024.
- [4] LHCb collaboration, R. Aaij *et al.*, *Simultaneous determination of CKM angle γ and charm mixing parameters*, JHEP **12** (2021) 141, [arXiv:2110.02350](#).
- [5] Y. Grossman and D. J. Robinson, *SU(3) sum rules for charm decay*, JHEP **04** (2013) 067, [arXiv:1211.3361](#).
- [6] E. Franco, S. Mishima, and L. Silvestrini, *The Standard Model confronts CP violation in $D^0 \rightarrow \pi^+ \pi^-$ and $D^0 \rightarrow K^+ K^-$* , JHEP **05** (2012) 140, [arXiv:1203.3131](#).
- [7] S. Müller, U. Nierste, and S. Schacht, *Sum rules of charm CP asymmetries beyond the $SU(3)_F$ limit*, Phys. Rev. Lett. **115** (2015) 251802, [arXiv:1506.04121](#).
- [8] A. Khodjamirian and A. A. Petrov, *Direct CP asymmetry in $D \rightarrow \pi^- \pi^+$ and $D \rightarrow K^- K^+$ in QCD-based approach*, Phys. Lett. **B774** (2017) 235, [arXiv:1706.07780](#).
- [9] H.-Y. Cheng and C.-W. Chiang, *Revisiting CP violation in $D \rightarrow PP$ and VP decays*, Phys. Rev. **D100** (2019) 093002, [arXiv:1909.03063](#).
- [10] Y. Grossman and S. Schacht, *The emergence of the $\Delta U = 0$ rule in charm physics*, JHEP **07** (2019) 020, [arXiv:1903.10952](#).
- [11] H.-Y. Cheng and C.-W. Chiang, *CP violation in quasi-two-body $D \rightarrow VP$ decays and three-body D decays mediated by vector resonances*, Phys. Rev. **D104** (2021) 073003, [arXiv:2104.13548](#).
- [12] S. Schacht and A. Soni, *Enhancement of charm CP violation due to nearby resonances*, Phys. Lett. **B825** (2022) 136855, [arXiv:2110.07619](#).
- [13] M. Gavrilova, Y. Grossman, and S. Schacht, *Determination of the $D \rightarrow \pi\pi$ ratio of penguin over tree diagrams*, Phys. Rev. **D109** (2024) 033011, [arXiv:2312.10140](#).
- [14] A. Pich, E. Solomonidi, and L. Vale Silva, *Final-state interactions in the CP asymmetries of charm-meson two-body decays*, Phys. Rev. **D108** (2023) 036026, [arXiv:2305.11951](#).
- [15] A. Lenz, M. L. Piscopo, and A. V. Rusov, *Two body non-leptonic D^0 decays from LCSR and implications for $\Delta a_{CP}^{\text{dir}}$* , JHEP **03** (2024) 151, [arXiv:2312.13245](#).

- [16] C. Bolognani, U. Nierste, S. Schacht, and K. K. Vos, *Anatomy of non-leptonic two-body decays of charmed mesons into final states with η'* , *JHEP* **05** (2025) 148, [arXiv:2410.08138](https://arxiv.org/abs/2410.08138).
- [17] A. Lenz and G. Wilkinson, *Mixing and CP violation in the charm system*, *Annu. Rev. Nucl. Part. Sci.* **71** (2021) 1, [arXiv:2011.04443](https://arxiv.org/abs/2011.04443).
- [18] T. Pajero, *Recent advances in charm mixing and CP violation at LHCb*, *Mod. Phys. Lett.* **A37** (2022) 2230012, [arXiv:2208.05769](https://arxiv.org/abs/2208.05769).
- [19] A. A. Petrov, *Charm physics*, *Eur. Phys. J. Spec. Top.* **233** (2024) 439.
- [20] Y. Grossman, A. L. Kagan, and Y. Nir, *New physics and CP violation in singly Cabibbo suppressed D decays*, *Phys. Rev.* **D75** (2007) 036008, [arXiv:hep-ph/0609178](https://arxiv.org/abs/hep-ph/0609178).
- [21] W. Altmannshofer, R. Primulando, C.-T. Yu, and F. Yu, *New physics models of direct CP violation in charm decays*, *JHEP* **04** (2012) 049, [arXiv:1202.2866](https://arxiv.org/abs/1202.2866).
- [22] A. Dery and Y. Nir, *Implications of the LHCb discovery of CP violation in charm decays*, *JHEP* **12** (2019) 104, [arXiv:1909.11242](https://arxiv.org/abs/1909.11242).
- [23] R. Bause, H. Gisbert, M. Golz, and G. Hiller, *Exploiting CP asymmetries in rare charm decays*, *Phys. Rev.* **D101** (2020) 115006, [arXiv:2004.01206](https://arxiv.org/abs/2004.01206).
- [24] A. J. Buras, P. Colangelo, F. De Fazio, and F. Loparco, *The charm of 331*, *JHEP* **10** (2021) 021, [arXiv:2107.10866](https://arxiv.org/abs/2107.10866).
- [25] R. Bause *et al.*, *U-spin-CP anomaly in charm*, *Phys. Rev.* **D108** (2023) 035005, [arXiv:2210.16330](https://arxiv.org/abs/2210.16330).
- [26] S. Iguro, U. Nierste, E. Overduin, and M. Schüßler, *SU(3)_F sum rules for CP asymmetries of D_(s) decays*, *Phys. Rev.* **D111** (2025) 035023, [arXiv:2408.03227](https://arxiv.org/abs/2408.03227).
- [27] Particle Data Group, S. Navas *et al.*, *Review of particle physics*, *Phys. Rev.* **D110** (2024) 030001.
- [28] C. P. Enz and R. R. Lewis, *On the phenomenological description of CP violation for K mesons and its consequences*, *Helv. Phys. Acta* **38** (1965) 860.
- [29] J. Brod, A. L. Kagan, and J. Zupan, *Size of direct CP violation in singly Cabibbo-suppressed D decays*, *Phys. Rev.* **D86** (2012) 014023, [arXiv:1111.5000](https://arxiv.org/abs/1111.5000).
- [30] H.-N. Li, C.-D. Lu, and F.-S. Yu, *Branching ratios and direct CP asymmetries in D → PP decays*, *Phys. Rev.* **D86** (2012) 036012, [arXiv:1203.3120](https://arxiv.org/abs/1203.3120).
- [31] U. Nierste and S. Schacht, *CP violation in D⁰ → K_SK_S*, *Phys. Rev.* **D92** (2015) 054036, [arXiv:1508.00074](https://arxiv.org/abs/1508.00074).
- [32] F. Buccella, A. Paul, and P. Santorelli, *SU(3)_F breaking through final state interactions and CP asymmetries in D → PP decays*, *Phys. Rev.* **D99** (2019) 113001, [arXiv:1902.05564](https://arxiv.org/abs/1902.05564).

- [33] CLEO collaboration, G. Bonvicini *et al.*, *Search for CP violation in $D^0 \rightarrow K_S^0\pi^0$ and $D^0 \rightarrow \pi^0\pi^0$ and $D^0 \rightarrow K_S^0K_S^0$ decays*, *Phys. Rev.* **D63** (2001) 071101, [arXiv:hep-ex/0012054](https://arxiv.org/abs/hep-ex/0012054).
- [34] LHCb collaboration, R. Aaij *et al.*, *Measurement of the time-integrated CP asymmetry in $D^0 \rightarrow K_S^0K_S^0$ decays*, *JHEP* **10** (2015) 055, [arXiv:1508.06087](https://arxiv.org/abs/1508.06087).
- [35] LHCb collaboration, R. Aaij *et al.*, *Measurement of CP asymmetry in $D^0 \rightarrow K_S^0K_S^0$ decays*, *Phys. Rev.* **D104** (2021) L031102, [arXiv:2105.01565](https://arxiv.org/abs/2105.01565).
- [36] CMS collaboration, A. Hayrapetyan *et al.*, *Search for CP violation in $D^0 \rightarrow K_S^0K_S^0$ decays in proton-proton collisions at $\sqrt{s} = 13$ TeV*, *Eur. Phys. J.* **C84** (2024) 1264, [arXiv:2405.11606](https://arxiv.org/abs/2405.11606).
- [37] Belle and Belle II collaborations, I. Adachi *et al.*, *Measurement of the time-integrated CP asymmetry in $D^0 \rightarrow K_S^0K_S^0$ decays using Belle and Belle II data*, *Phys. Rev.* **D111** (2025) 012015, [arXiv:2411.00306](https://arxiv.org/abs/2411.00306).
- [38] Belle and Belle II collaborations, I. Adachi *et al.*, *Measurement of the time-integrated CP asymmetry in $D^0 \rightarrow K_S^0K_S^0$ decays using opposite-side flavor tagging at Belle and Belle II*, [arXiv:2504.15881](https://arxiv.org/abs/2504.15881).
- [39] T. Pajero and M. J. Morello, CHARMFITTER, <https://github.com/tpajero/charm-fitter>.
- [40] T. Pajero and M. J. Morello, *Mixing and CP violation in $D^0 \rightarrow K^-\pi^+$ decays*, *JHEP* **03** (2022) 162, [arXiv:2106.02014](https://arxiv.org/abs/2106.02014).
- [41] LHCb collaboration, *LHCb Trigger and Online Upgrade Technical Design Report*, CERN-LHCC-2014-016, 2014.
- [42] LHCb collaboration, *LHCb Upgrade GPU High Level Trigger Technical Design Report*, CERN-LHCC-2020-006, 2020.
- [43] LHCb collaboration, R. Aaij *et al.*, *Measurement of D^0 - \bar{D}^0 mixing and search for CP violation with $D^0 \rightarrow K^+\pi^-$ decays*, *Phys. Rev.* **D111** (2025) 012001, [arXiv:2407.18001](https://arxiv.org/abs/2407.18001).
- [44] LHCb collaboration, R. Aaij *et al.*, *The LHCb Upgrade I*, *JINST* **19** (2024) P05065, [arXiv:2305.10515](https://arxiv.org/abs/2305.10515).
- [45] LHCb collaboration, A. A. Alves Jr. *et al.*, *The LHCb detector at the LHC*, *JINST* **3** (2008) S08005.
- [46] LHCb collaboration, *LHCb VELO Upgrade Technical Design Report*, CERN-LHCC-2013-021, 2013.
- [47] LHCb collaboration, *LHCb Tracker Upgrade Technical Design Report*, CERN-LHCC-2014-001, 2014.
- [48] LHCb collaboration, *LHCb PID Upgrade Technical Design Report*, CERN-LHCC-2013-022, 2013.

- [49] T. Sjöstrand, S. Mrenna, and P. Skands, *A brief introduction to PYTHIA 8.1*, *Comput. Phys. Commun.* **178** (2008) 852, [arXiv:0710.3820](https://arxiv.org/abs/0710.3820).
- [50] I. Belyaev *et al.*, *Handling of the generation of primary events in Gauss, the LHCb simulation framework*, *J. Phys. Conf. Ser.* **331** (2011) 032047.
- [51] D. J. Lange, *The EvtGen particle decay simulation package*, *Nucl. Instrum. Meth. A* **462** (2001) 152.
- [52] N. Davidson, T. Przedzinski, and Z. Was, *PHOTOS interface in C++: Technical and physics documentation*, *Comput. Phys. Commun.* **199** (2016) 86, [arXiv:1011.0937](https://arxiv.org/abs/1011.0937).
- [53] Geant4 collaboration, J. Allison *et al.*, *Geant4 developments and applications*, *IEEE Trans. Nucl. Sci.* **53** (2006) 270.
- [54] M. Clemencic *et al.*, *The LHCb simulation application, Gauss: Design, evolution and experience*, *J. Phys. Conf. Ser.* **331** (2011) 032023.
- [55] LHCb collaboration, R. Aaij *et al.*, *Search for time-dependent CP violation in $D^0 \rightarrow K^+ K^-$ and $D^0 \rightarrow \pi^+ \pi^-$ decays*, *Phys. Rev. D* **104** (2021) 072010, [arXiv:2105.09889](https://arxiv.org/abs/2105.09889).
- [56] L. Pica, *Charm CP violation measurements with K_S^0 final states at LHCb*, 2025, PhD thesis, Scuola Normale Superiore, Pisa, Italy.
- [57] T. Hastie, R. Tibshirani, and J. Friedman, *The elements of statistical learning*, Springer, 2009.
- [58] N. L. Johnson, *Systems of frequency curves generated by methods of translation*, *Biometrika* **36** (1949) 149.

LHCb collaboration

R. Aaij³⁸ , A.S.W. Abdelmotteleb⁵⁷ , C. Abellan Beteta⁵¹ , F. Abudinén⁵⁷ , T. Ackernley⁶¹ , A. A. Adefisoye⁶⁹ , B. Adeva⁴⁷ , M. Adinolfi⁵⁵ , P. Adlarson⁸⁵ , C. Agapopoulou¹⁴ , C.A. Aidala⁸⁷ , Z. Ajaltouni¹¹ , S. Akar¹¹ , K. Akiba³⁸ , M. Akthar⁴⁰ , P. Albicocco²⁸ , J. Albrecht^{19,g} , R. Aleksiejunas⁸⁰ , F. Alessio⁴⁹ , P. Alvarez Cartelle⁵⁶ , R. Amalric¹⁶ , S. Amato³ , J.L. Amey⁵⁵ , Y. Amhis¹⁴ , L. An⁶ , L. Anderlini²⁷ , M. Andersson⁵¹ , P. Andreola⁵¹ , M. Andreotti²⁶ , S. Andres Estrada⁸⁴ , A. Anelli^{31,p,49} , D. Ao⁷ , C. Arata¹² , F. Archilli^{37,w} , Z. Areg⁶⁹ , M. Argenton²⁶ , S. Arguedas Cuendis^{9,49} , L. Arnone^{31,p} , A. Artamonov⁴⁴ , M. Artuso⁶⁹ , E. Aslanides¹³ , R. Ataíde Da Silva⁵⁰ , M. Atzeni⁶⁵ , B. Audurier¹² , J. A. Authier¹⁵ , D. Bacher⁶⁴ , I. Bachiller Perea⁵⁰ , S. Bachmann²² , M. Bachmayer⁵⁰ , J.J. Back⁵⁷ , P. Baladron Rodriguez⁴⁷ , V. Balagura¹⁵ , A. Balboni²⁶ , W. Baldini²⁶ , Z. Baldwin⁷⁸ , L. Balzani¹⁹ , H. Bao⁷ , J. Baptista de Souza Leite² , C. Barbero Pretel^{47,12} , M. Barbetti²⁷ , I. R. Barbosa⁷⁰ , R.J. Barlow⁶³ , M. Barnyakov²⁵ , S. Barsuk¹⁴ , W. Barter⁵⁹ , J. Bartz⁶⁹ , S. Bashir⁴⁰ , B. Batsukh⁵ , P. B. Battista¹⁴ , A. Bay⁵⁰ , A. Beck⁶⁵ , M. Becker¹⁹ , F. Bedeschchi³⁵ , I.B. Bediaga² , N. A. Behling¹⁹ , S. Belin⁴⁷ , A. Bellavista²⁵ , K. Belous⁴⁴ , I. Belov²⁹ , I. Belyaev³⁶ , G. Benane¹³ , G. Bencivenni²⁸ , E. Ben-Haim¹⁶ , A. Berezhnoy⁴⁴ , R. Bernet⁵¹ , S. Bernet Andres⁴⁶ , A. Bertolin³³ , C. Betancourt⁵¹ , F. Betti⁵⁹ , J. Bex⁵⁶ , Ia. Bezshyiko⁵¹ , O. Bezshykyo⁸⁶ , J. Bhom⁴¹ , M.S. Bieker¹⁸ , N.V. Biesuz²⁶ , A. Biolchini³⁸ , M. Birch⁶² , F.C.R. Bishop¹⁰ , A. Bitadze⁶³ , A. Bizzeti^{27,q} , T. Blake^{57,c} , F. Blanc⁵⁰ , J.E. Blank¹⁹ , S. Blusk⁶⁹ , V. Bocharnikov⁴⁴ , J.A. Boelhauve¹⁹ , O. Boente Garcia¹⁵ , T. Boettcher⁶⁸ , A. Bohare⁵⁹ , A. Boldyrev⁴⁴ , C.S. Bolognani⁸² , R. Bolzonella^{26,m} , R. B. Bonacci¹ , N. Bondar^{44,49} , A. Bordelius⁴⁹ , F. Borgato^{33,49} , S. Borghi⁶³ , M. Borsato^{31,p} , J.T. Borsuk⁸³ , E. Bottalico⁶¹ , S.A. Bouchiba⁵⁰ , M. Bovill⁶⁴ , T.J.V. Bowcock⁶¹ , A. Boyer⁴⁹ , C. Bozzi²⁶ , J. D. Brandenburg⁸⁸ , A. Brea Rodriguez⁵⁰ , N. Breer¹⁹ , J. Brodzicka⁴¹ , A. Brossa Gonzalo^{47,†} , J. Brown⁶¹ , D. Brundu³² , E. Buchanan⁵⁹ , M. Burgos Marcos⁸² , A.T. Burke⁶³ , C. Burr⁴⁹ , E. Butera³⁵ , C. Buti²⁷ , J.S. Butter⁵⁶ , J. Buytaert⁴⁹ , W. Byczynski⁴⁹ , S. Cadeddu³² , H. Cai⁷⁵ , Y. Cai⁵ , A. Caillet¹⁶ , R. Calabrese^{26,m} , S. Calderon Ramirez⁹ , L. Calefice⁴⁵ , M. Calvi^{31,p} , M. Calvo Gomez⁴⁶ , P. Camargo Magalhaes^{2,a} , J. I. Cambon Bouzas⁴⁷ , P. Campana²⁸ , D.H. Campora Perez⁸² , A.F. Campoverde Quezada⁷ , S. Capelli³¹ , M. Caporale²⁵ , L. Capriotti²⁶ , R. Caravaca-Mora⁹ , A. Carbone^{25,k} , L. Carcedo Salgado⁴⁷ , R. Cardinale^{29,n} , A. Cardini³² , P. Carniti³¹ , L. Carus²² , A. Casais Vidal⁶⁵ , R. Caspary²² , G. Casse⁶¹ , M. Cattaneo⁴⁹ , G. Cavallero²⁶ , V. Cavallini^{26,m} , S. Celani²² , I. Celestino^{35,t} , S. Cesare^{30,o} , A.J. Chadwick⁶¹ , I. Chahrour⁸⁷ , H. Chang^{4,d} , M. Charles¹⁶ , Ph. Charpentier⁴⁹ , E. Chatzianagnostou³⁸ , R. Cheaib⁷⁹ , M. Chefdeville¹⁰ , C. Chen⁵⁶ , J. Chen⁵⁰ , S. Chen⁵ , Z. Chen⁷ , M. Cherif¹² , A. Chernov⁴¹ , S. Chernyshenko⁵³ , X. Chiropoulos⁸² , V. Chobanova⁸⁴ , M. Chrzaszcz⁴¹ , A. Chubykin⁴⁴ , V. Chulikov^{28,36,49} , P. Ciambrone²⁸ , X. Cid Vidal⁴⁷ , G. Ciezarek⁴⁹ , P. Cifra³⁸ , P.E.L. Clarke⁵⁹ , M. Clemencic⁴⁹ , H.V. Cliff⁵⁶ , J. Closier⁴⁹ , C. Cocha Toapaxi²² , V. Coco⁴⁹ , J. Cogan¹³ , E. Cogneras¹¹ , L. Cojocariu⁴³ , S. Collavitti⁵⁰ , P. Collins⁴⁹ , T. Colombo⁴⁹ , M. Colonna¹⁹ , A. Comerma-Montells⁴⁵ , L. Congedo²⁴ , J. Connaughton⁵⁷ , A. Contu³² , N. Cooke⁶⁰ , G. Cordova^{35,t} , C. Coronel⁶⁶ , I. Corredoira¹² , A. Correia¹⁶ , G. Corti⁴⁹ , J. Cottee Meldrum⁵⁵ , B. Couturier⁴⁹ , D.C. Craik⁵¹ , M. Cruz Torres^{2,h} , E. Curras Rivera⁵⁰ , R. Currie⁵⁹ , C.L. Da Silva⁶⁸ , S. Dadabaev⁴⁴ , L. Dai⁷² , X. Dai⁴ , E. Dall'Occo⁴⁹ , J. Dalseno⁸⁴ , C. D'Ambrosio⁶² , J. Daniel¹¹

P. d'Argent²⁴ , G. Darze³ , A. Davidson⁵⁷ , J.E. Davies⁶³ , O. De Aguiar Francisco⁶³ , C. De Angelis^{32,l} , F. De Benedetti⁴⁹ , J. de Boer³⁸ , K. De Bruyn⁸¹ , S. De Capua⁶³ , M. De Cian^{63,49} , U. De Freitas Carneiro Da Graca^{2,b} , E. De Lucia²⁸ , J.M. De Miranda² , L. De Paula³ , M. De Serio^{24,i} , P. De Simone²⁸ , F. De Vellis¹⁹ , J.A. de Vries⁸² , F. Debernardis²⁴ , D. Decamp¹⁰ , S. Dekkers¹ , L. Del Buono¹⁶ , B. Delaney⁶⁵ , H.-P. Dembinski¹⁹ , J. Deng⁸ , V. Denysenko⁵¹ , O. Deschamps¹¹ , F. Dettori^{32,l} , B. Dey⁷⁹ , P. Di Nezza²⁸ , I. Diachkov⁴⁴ , S. Didenko⁴⁴ , S. Ding⁶⁹ , Y. Ding⁵⁰ , L. Dittmann²² , V. Dobishuk⁵³ , A. D. Docheva⁶⁰ , A. Doheny⁵⁷ , C. Dong^{4,d} , A.M. Donohoe²³ , F. Dordei³² , A.C. dos Reis² , A. D. Dowling⁶⁹ , L. Dreyfus¹³ , W. Duan⁷³ , P. Duda⁸³ , L. Dufour⁴⁹ , V. Duk³⁴ , P. Durante⁴⁹ , M. Duras⁸³ , J.M. Durham⁶⁸ , O. D. Durmus⁷⁹ , A. Dziurda⁴¹ , A. Dzyuba⁴⁴ , S. Easo⁵⁸ , E. Eckstein¹⁸ , U. Egede¹ , A. Egorychev⁴⁴ , V. Egorychev⁴⁴ , S. Eisenhardt⁵⁹ , E. Ejopu⁶¹ , L. Eklund⁸⁵ , M. Elashri⁶⁶ , J. Ellbracht¹⁹ , S. Ely⁶² , A. Ene⁴³ , J. Eschle⁶⁹ , S. Esen²² , T. Evans³⁸ , F. Fabiano³² , S. Faghih⁶⁶ , L.N. Falcao² , B. Fang⁷ , R. Fantechi³⁵ , L. Fantini^{34,s} , M. Faria⁵⁰ , K. Farmer⁵⁹ , D. Fazzini^{31,p} , L. Felkowski⁸³ , M. Feng^{5,7} , M. Feo¹⁹ , A. Fernandez Casani⁴⁸ , M. Fernandez Gomez⁴⁷ , A.D. Fernez⁶⁷ , F. Ferrari^{25,k} , F. Ferreira Rodrigues³ , M. Ferrillo⁵¹ , M. Ferro-Luzzi⁴⁹ , S. Filippov⁴⁴ , R.A. Fini²⁴ , M. Fiorini^{26,m} , M. Firlej⁴⁰ , K.L. Fischer⁶⁴ , D.S. Fitzgerald⁸⁷ , C. Fitzpatrick⁶³ , T. Fiutowski⁴⁰ , F. Fleuret¹⁵ , A. Fomin⁵² , M. Fontana²⁵ , L. A. Foreman⁶³ , R. Forty⁴⁹ , D. Foulds-Holt⁵⁹ , V. Franco Lima³ , M. Franco Sevilla⁶⁷ , M. Frank⁴⁹ , E. Franzoso^{26,m} , G. Frau⁶³ , C. Frei⁴⁹ , D.A. Friday^{63,49} , J. Fu⁷ , Q. Führing^{19,g,56} , T. Fulghesu¹³ , G. Galati²⁴ , M.D. Galati³⁸ , A. Gallas Torreira⁴⁷ , D. Galli^{25,k} , S. Gambetta⁵⁹ , M. Gandelman³ , P. Gandini³⁰ , B. Ganie⁶³ , H. Gao⁷ , R. Gao⁶⁴ , T.Q. Gao⁵⁶ , Y. Gao⁸ , Y. Gao⁶ , Y. Gao⁸ , L.M. Garcia Martin⁵⁰ , P. Garcia Moreno⁴⁵ , J. García Pardiñas⁶⁵ , P. Gardner⁶⁷ , K. G. Garg⁸ , L. Garrido⁴⁵ , C. Gaspar⁴⁹ , A. Gavrikov³³ , L.L. Gerken¹⁹ , E. Gersabeck²⁰ , M. Gersabeck²⁰ , T. Gershon⁵⁷ , S. Ghizzo^{29,n} , Z. Ghorbanimoghaddam⁵⁵ , F. I. Giasemis^{16,f} , V. Gibson⁵⁶ , H.K. Giemza⁴² , A.L. Gilman⁶⁶ , M. Giovannetti²⁸ , A. Gioventù⁴⁵ , L. Girardey^{63,58} , M.A. Giza⁴¹ , F.C. Glaser^{14,22} , V.V. Gligorov¹⁶ , C. Göbel⁷⁰ , L. Golinka-Bezshyyko⁸⁶ , E. Golobardes⁴⁶ , D. Golubkov⁴⁴ , A. Golutvin^{62,49} , S. Gomez Fernandez⁴⁵ , W. Gomulka⁴⁰ , I. Gonçales Vaz⁴⁹ , F. Goncalves Abrantes⁶⁴ , M. Goncerz⁴¹ , G. Gong^{4,d} , J. A. Gooding¹⁹ , I.V. Gorelov⁴⁴ , C. Gotti³¹ , E. Govorkova⁶⁵ , J.P. Grabowski³⁰ , L.A. Granado Cardoso⁴⁹ , E. Graugés⁴⁵ , E. Graverini^{50,u} , L. Grazette⁵⁷ , G. Graziani²⁷ , A. T. Grecu⁴³ , N.A. Grieser⁶⁶ , L. Grillo⁶⁰ , S. Gromov⁴⁴ , C. Gu¹⁵ , M. Guarise²⁶ , L. Guerry¹¹ , V. Guliaeva⁴⁴ , P. A. Günther²² , A.-K. Guseinov⁵⁰ , E. Gushchin⁴⁴ , Y. Guz^{6,49} , T. Gys⁴⁹ , K. Habermann¹⁸ , T. Hadavizadeh¹ , C. Hadjivasiliou⁶⁷ , G. Haefeli⁵⁰ , C. Haen⁴⁹ , S. Haken⁵⁶ , G. Hallett⁵⁷ , P.M. Hamilton⁶⁷ , J. Hammerich⁶¹ , Q. Han³³ , X. Han^{22,49} , S. Hansmann-Menzemer²² , L. Hao⁷ , N. Harnew⁶⁴ , T. H. Harris¹ , M. Hartmann¹⁴ , S. Hashmi⁴⁰ , J. He^{7,e} , A. Hedes⁶³ , F. Hemmer⁴⁹ , C. Henderson⁶⁶ , R. Henderson¹⁴ , R.D.L. Henderson¹ , A.M. Hennequin⁴⁹ , K. Hennessy⁶¹ , L. Henry⁵⁰ , J. Herd⁶² , P. Herrero Gascon²² , J. Heuel¹⁷ , A. Heyn¹³ , A. Hicheur³ , G. Hijano Mendizabal⁵¹ , J. Horswill⁶³ , R. Hou⁸ , Y. Hou¹¹ , D. C. Houston⁶⁰ , N. Howarth⁶¹ , J. Hu⁷³ , W. Hu⁷ , X. Hu^{4,d} , W. Hulsbergen³⁸ , R.J. Hunter⁵⁷ , M. Hushchyn⁴⁴ , D. Hutchcroft⁶¹ , M. Idzik⁴⁰ , D. Ilin⁴⁴ , P. Ilten⁶⁶ , A. Iniuikhin⁴⁴ , A. Iohner¹⁰ , A. Ishteev⁴⁴ , K. Ivshin⁴⁴ , H. Jage¹⁷ , S.J. Jaimes Elles^{77,48,49} , S. Jakobsen⁴⁹ , E. Jans³⁸ , B.K. Jashal⁴⁸ , A. Jawahery⁶⁷ , C. Jayaweera⁵⁴ , V. Jevtic¹⁹ , Z. Jia¹⁶ , E. Jiang⁶⁷ , X. Jiang^{5,7} , Y. Jiang⁷ , Y. J. Jiang⁶

E. Jimenez Moya⁹ , N. Jindal⁸⁸ , M. John⁶⁴ , A. John Rubesh Rajan²³ ,
 D. Johnson⁵⁴ , C.R. Jones⁵⁶ , S. Joshi⁴² , B. Jost⁴⁹ , J. Juan Castella⁵⁶ , N. Jurik⁴⁹ ,
 I. Juszczak⁴¹ , D. Kaminaris⁵⁰ , S. Kandybei⁵² , M. Kane⁵⁹ , Y. Kang^{4,d} , C. Kar¹¹ ,
 M. Karacson⁴⁹ , A. Kauniskangas⁵⁰ , J.W. Kautz⁶⁶ , M.K. Kazanecki⁴¹ , F. Keizer⁴⁹ ,
 M. Kenzie⁵⁶ , T. Ketel³⁸ , B. Khanji⁶⁹ , A. Kharisova⁴⁴ , S. Kholodenko^{62,49} ,
 G. Khreich¹⁴ , T. Kirn¹⁷ , V.S. Kirsebom^{31,p} , O. Kitouni⁶⁵ , S. Klaver³⁹ ,
 N. Kleijne^{35,t} , D. K. Klekots⁸⁶ , K. Klimaszewski⁴² , M.R. Kmiec⁴² , T. Knospe¹⁹ ,
 R. Kolb²² , S. Koliiev⁵³ , L. Kolk¹⁹ , A. Konoplyannikov⁶ , P. Kopciewicz⁴⁹ ,
 P. Koppenburg³⁸ , A. Korchin⁵² , M. Korolev⁴⁴ , I. Kostiuk³⁸ , O. Kot⁵³ ,
 S. Kotriakhova , E. Kowalczyk⁶⁷ , A. Kozachuk⁴⁴ , P. Kravchenko⁴⁴ , L. Kravchuk⁴⁴ ,
 O. Kravcov⁸⁰ , M. Kreps⁵⁷ , P. Krokovny⁴⁴ , W. Krupa⁶⁹ , W. Krzemien⁴² ,
 O. Kshyvanskyi⁵³ , S. Kubis⁸³ , M. Kucharczyk⁴¹ , V. Kudryavtsev⁴⁴ , E. Kulikova⁴⁴ ,
 A. Kupsc⁸⁵ , V. Kushnir⁵² , B. Kutsenko¹³ , J. Kvapil⁶⁸ , I. Kyryllin⁵² ,
 D. Lacarrere⁴⁹ , P. Laguarta Gonzalez⁴⁵ , A. Lai³² , A. Lampis³² , D. Lancierini⁶² ,
 C. Landesa Gomez⁴⁷ , J.J. Lane¹ , G. Lanfranchi²⁸ , C. Langenbruch²² , J. Langer¹⁹ ,
 O. Lantwin⁴⁴ , T. Latham⁵⁷ , F. Lazzari^{35,u,49} , C. Lazzeroni⁵⁴ , R. Le Gac¹³ , H. Lee⁶¹ , R. Lefèvre¹¹ , A. Leflat⁴⁴ , S. Legotin⁴⁴ , M. Lehuraux⁵⁷ , E. Lemos Cid⁴⁹ ,
 O. Leroy¹³ , T. Lesiak⁴¹ , E. D. Lesser⁴⁹ , B. Leverington²² , A. Li^{4,d} , C. Li^{4,d} , C. Li¹³ , H. Li⁷³ , J. Li⁸ , K. Li⁷⁶ , L. Li⁶³ , M. Li⁸ , P. Li⁷ , P.-R. Li⁷⁴ , Q. Li^{5,7} , T. Li⁷² , T. Li⁷³ , Y. Li⁸ , Y. Li⁵ , Y. Li⁴ , Z. Lian^{4,d} , Q. Liang⁸ , X. Liang⁶⁹ , Z. Liang³² , S. Libralon⁴⁸ , A. L. Lightbody¹² , C. Lin⁷ , T. Lin⁵⁸ , R. Lindner⁴⁹ , H. Linton⁶² , R. Litvinov³² , D. Liu⁸ , F. L. Liu¹ , G. Liu⁷³ , K. Liu⁷⁴ , S. Liu^{5,7} , W. Liu⁸ , Y. Liu⁵⁹ , Y. Liu⁷⁴ , Y. L. Liu⁶² , G. Loachamin Ordóñez⁷⁰ ,
 A. Lobo Salvia⁴⁵ , A. Loi³² , T. Long⁵⁶ , F. C. L. Lopes^{2,a} , J.H. Lopes³ ,
 A. Lopez Huertas⁴⁵ , C. Lopez Iribarne⁴⁷ , S. López Soliño⁴⁷ , Q. Lu¹⁵ ,
 C. Lucarelli⁴⁹ , D. Lucchesi^{33,r} , M. Lucio Martinez⁴⁸ , Y. Luo⁶ , A. Lupato^{33,j} ,
 E. Luppi^{26,m} , K. Lynch²³ , X.-R. Lyu⁷ , G. M. Ma^{4,d} , H. Ma⁷² , S. Maccolini¹⁹ ,
 F. Machefert¹⁴ , F. Maciuc⁴³ , B. Mack⁶⁹ , I. Mackay⁶⁴ , L. M. Mackey⁶⁹ ,
 L.R. Madhan Mohan⁵⁶ , M. J. Madurai⁵⁴ , D. Magdalinski³⁸ , D. Maisuzenko⁴⁴ ,
 J.J. Malczewski⁴¹ , S. Malde⁶⁴ , L. Malentacca⁴⁹ , A. Malinin⁴⁴ , T. Maltsev⁴⁴ ,
 G. Manca^{32,l} , G. Mancinelli¹³ , C. Mancuso¹⁴ , R. Manera Escalero⁴⁵ , F. M. Manganella³⁷ , D. Manuzzi²⁵ , D. Marangotto^{30,o} , J.F. Marchand¹⁰ ,
 R. Marchevski⁵⁰ , U. Marconi²⁵ , E. Mariani¹⁶ , S. Mariani⁴⁹ , C. Marin Benito⁴⁵ ,
 J. Marks²² , A.M. Marshall⁵⁵ , L. Martel⁶⁴ , G. Martelli³⁴ , G. Martellotti³⁶ ,
 L. Martinazzoli⁴⁹ , M. Martinelli^{31,p} , D. Martinez Gomez⁸¹ , D. Martinez Santos⁸⁴ ,
 F. Martinez Vidal⁴⁸ , A. Martorell i Granollers⁴⁶ , A. Massafferri² , R. Matev⁴⁹ ,
 A. Mathad⁴⁹ , V. Matiunin⁴⁴ , C. Matteuzzi⁶⁹ , K.R. Mattioli¹⁵ , A. Mauri⁶² ,
 E. Maurice¹⁵ , J. Mauricio⁴⁵ , P. Mayencourt⁵⁰ , J. Mazorra de Cos⁴⁸ , M. Mazurek⁴² ,
 M. McCann⁶² , T.H. McGrath⁶³ , N.T. McHugh⁶⁰ , A. McNab⁶³ , R. McNulty²³ ,
 B. Meadows⁶⁶ , G. Meier¹⁹ , D. Melnychuk⁴² , D. Mendoza Granada¹⁶ , P. Menendez Valdes Perez⁴⁷ , F. M. Meng^{4,d} , M. Merk^{38,82} , A. Merli^{50,30} ,
 L. Meyer Garcia⁶⁷ , D. Miao^{5,7} , H. Miao⁷ , M. Mikhasenko⁷⁸ , D.A. Milanes^{77,z} ,
 A. Minotti^{31,p} , E. Minucci²⁸ , T. Miralles¹¹ , B. Mitreska¹⁹ , D.S. Mitzel¹⁹ , R. Mocanu⁴³ , A. Modak⁵⁸ , L. Moeser¹⁹ , R.D. Moise¹⁷ , E. F. Molina Cardenas⁸⁷ ,
 T. Mombächer⁴⁹ , M. Monk^{57,1} , S. Monteil¹¹ , A. Morcillo Gomez⁴⁷ , G. Morello²⁸ ,
 M.J. Morello^{35,t} , M.P. Morgenthaler²² , A. Moro^{31,p} , J. Moron⁴⁰ , W. Morren³⁸ ,
 A.B. Morris⁴⁹ , A.G. Morris¹³ , R. Mountain⁶⁹ , H. Mu^{4,d} , Z. M. Mu⁶ ,
 E. Muhammad⁵⁷ , F. Muheim⁵⁹ , M. Mulder⁸¹ , K. Müller⁵¹ , F. Muñoz-Rojas⁹ ,
 R. Murta⁶² , V. Mytrochenko⁵² , P. Naik⁶¹ , T. Nakada⁵⁰ , R. Nandakumar⁵⁸ ,
 T. Nanut⁴⁹ , I. Nasteva³ , M. Needham⁵⁹ , E. Nekrasova⁴⁴ , N. Neri^{30,o} <img alt="ORCID icon" data-bbox="10000 91 10

S. Neubert¹⁸ , N. Neufeld⁴⁹ , P. Neustroev⁴⁴, J. Nicolini⁴⁹ , D. Nicotra⁸² , E.M. Niel¹⁵ , N. Nikitin⁴⁴ , L. Nisi¹⁹ , Q. Niu⁷⁴ , P. Nogarolli³ , P. Nogga¹⁸ , C. Normand⁵⁵ , J. Novoa Fernandez⁴⁷ , G. Nowak⁶⁶ , C. Nunez⁸⁷ , H. N. Nur⁶⁰ , A. Oblakowska-Mucha⁴⁰ , V. Obraztsov⁴⁴ , T. Oeser¹⁷ , A. Okhotnikov⁴⁴, O. Okhrimenko⁵³ , R. Oldeman^{32,l} , F. Oliva^{59,49} , E. Olivart Pino⁴⁵ , M. Olocco¹⁹ , C.J.G. Onderwater⁸² , R.H. O'Neil⁴⁹ , J.S. Ordonez Soto¹¹ , D. Osthuus¹⁹ , J.M. Otalora Goicochea³ , P. Owen⁵¹ , A. Oyanguren⁴⁸ , O. Ozcelik⁴⁹ , F. Paciolla^{35,x} , A. Padde⁴² , K.O. Paddeken¹⁸ , B. Pagare⁴⁷ , T. Pajero⁴⁹ , A. Palano²⁴ , L. Palini³⁰ , M. Palutan²⁸ , C. Pan⁷⁵ , X. Pan^{4,d} , S. Panebianco¹² , G. Panshin⁵ , L. Paolucci⁶³ , A. Papanestis⁵⁸ , M. Pappagallo^{24,i} , L.L. Pappalardo²⁶ , C. Pappenheimer⁶⁶ , C. Parkes⁶³ , D. Parmar⁷⁸ , B. Passalacqua^{26,m} , G. Passaleva²⁷ , D. Passaro^{35,t,49} , A. Pastore²⁴ , M. Patel⁶² , J. Patoc⁶⁴ , C. Patrignani^{25,k} , A. Paul⁶⁹ , C.J. Pawley⁸² , A. Pellegrino³⁸ , J. Peng^{5,7} , X. Peng⁷⁴, M. Pepe Altarelli²⁸ , S. Perazzini²⁵ , D. Pereima⁴⁴ , H. Pereira Da Costa⁶⁸ , M. Pereira Martinez⁴⁷ , A. Pereiro Castro⁴⁷ , C. Perez⁴⁶ , P. Perret¹¹ , A. Perrevoort⁸¹ , A. Perro^{49,13} , M.J. Peters⁶⁶ , K. Petridis⁵⁵ , A. Petrolini^{29,n} , S. Pezzulo^{29,n} , J. P. Pfaller⁶⁶ , H. Pham⁶⁹ , L. Pica^{35,t} , M. Piccini³⁴ , L. Piccolo³² , B. Pietrzek¹⁰ , G. Pietrzek¹⁴ , R. N. Pilato⁶¹ , D. Pinci³⁶ , F. Pisani⁴⁹ , M. Pizzichemi^{31,p,49} , V. M. Placinta⁴³ , M. Plo Casasus⁴⁷ , T. Poeschl⁴⁹ , F. Polci¹⁶ , M. Poli Lener²⁸ , A. Poluektov¹³ , N. Polukhina⁴⁴ , I. Polyakov⁶³ , E. Polycarpo³ , S. Ponce⁴⁹ , D. Popov^{7,49} , S. Poslavskii⁴⁴ , K. Prasant⁵⁹ , C. Prouve⁸⁴ , D. Provenzano^{32,l,49} , V. Pugatch⁵³ , G. Punzi^{35,u} , J.R. Pybus⁶⁸ , S. Qasim⁵¹ , Q. Q. Qian⁶ , W. Qian⁷ , N. Qin^{4,d} , S. Qu^{4,d} , R. Quagliani⁴⁹ , R.I. Rabadan Trejo⁵⁷ , R. Racz⁸⁰ , J.H. Rademacker⁵⁵ , M. Rama³⁵ , M. Ramírez García⁸⁷ , V. Ramos De Oliveira⁷⁰ , M. Ramos Pernas⁵⁷ , M.S. Rangel³ , F. Ratnikov⁴⁴ , G. Raven³⁹ , M. Rebollo De Miguel⁴⁸ , F. Redi^{30,j} , J. Reich⁵⁵ , F. Reiss²⁰ , Z. Ren⁷ , P.K. Resmi⁶⁴ , M. Ribalda Galvez⁴⁵ , R. Ribatti⁵⁰ , G. Ricart^{15,12} , D. Riccardi^{35,t} , S. Ricciardi⁵⁸ , K. Richardson⁶⁵ , M. Richardson-Slipper⁵⁶ , K. Rinnert⁶¹ , P. Robbe^{14,49} , G. Robertson⁶⁰ , E. Rodrigues⁶¹ , A. Rodriguez Alvarez⁴⁵ , E. Rodriguez Fernandez⁴⁷ , J.A. Rodriguez Lopez⁷⁷ , E. Rodriguez Rodriguez⁴⁹ , J. Roensch¹⁹ , A. Rogachev⁴⁴ , A. Rogovskiy⁵⁸ , D.L. Rolf¹⁹ , P. Roloff⁴⁹ , V. Romanovskiy⁶⁶ , A. Romero Vidal⁴⁷ , G. Romolini^{26,49} , F. Ronchetti⁵⁰ , T. Rong⁶ , M. Rotondo²⁸ , S. R. Roy²² , M.S. Rudolph⁶⁹ , M. Ruiz Diaz²² , R.A. Ruiz Fernandez⁴⁷ , J. Ruiz Vidal⁸² , J. Saavedra-Arias⁹ , J.J. Saborido Silva⁴⁷ , S. E. R. Sacha Emile R.⁴⁹ , N. Sagidova⁴⁴ , D. Sahoo⁷⁹ , N. Sahoo⁵⁴ , B. Saitta^{32,l} , M. Salomoni^{31,49,p} , I. Sanderswood⁴⁸ , R. Santacesaria³⁶ , C. Santamarina Rios⁴⁷ , M. Santimaria²⁸ , L. Santoro² , E. Santovetti³⁷ , A. Saputi^{26,49} , D. Saranin⁴⁴ , A. Sarnatskiy⁸¹ , G. Sarpis⁴⁹ , M. Sarpis⁸⁰ , C. Satriano^{36,v} , A. Satta³⁷ , M. Saur⁷⁴ , D. Savrina⁴⁴ , H. Sazak¹⁷ , F. Sborzacchi^{49,28} , A. Scarabotto¹⁹ , S. Schael¹⁷ , S. Scherl⁶¹ , M. Schiller²² , H. Schindler⁴⁹ , M. Schmelling²¹ , B. Schmidt⁴⁹ , N. Schmidt⁶⁸ , S. Schmitt⁶⁵ , H. Schmitz¹⁸, O. Schneider⁵⁰ , A. Schopper⁶² , N. Schulte¹⁹ , M.H. Schunke¹⁴ , G. Schwering¹⁷ , B. Sciascia²⁸ , A. Sciuccati⁴⁹ , G. Scriven⁸² , I. Segal⁷⁸ , S. Sellam⁴⁷ , A. Semennikov⁴⁴ , T. Senger⁵¹ , M. Senghi Soares³⁹ , A. Sergi^{29,n,49} , N. Serra⁵¹ , L. Sestini²⁷ , A. Seuthe¹⁹ , B. Sevilla Sanjuan⁴⁶ , Y. Shang⁶ , D.M. Shangase⁸⁷ , M. Shapkin⁴⁴ , R. S. Sharma⁶⁹ , I. Shchemerov⁴⁴ , L. Shchutska⁵⁰ , T. Shears⁶¹ , L. Shekhtman⁴⁴ , Z. Shen³⁸ , S. Sheng^{5,7} , V. Shevchenko⁴⁴ , B. Shi⁷ , Q. Shi⁷ , W. S. Shi⁷³ , Y. Shimizu¹⁴ , E. Shmanin²⁵ , R. Shorkin⁴⁴ , J.D. Shupperd⁶⁹ , R. Silva Coutinho² , G. Simi^{33,r} , S. Simone^{24,i} , M. Singha⁷⁹ , N. Skidmore⁵⁷ , T. Skwarnicki⁶⁹ , M.W. Slater⁵⁴ , E. Smith⁶⁵ , K. Smith⁶⁸ , M. Smith⁶² , L. Soares Lavra⁵⁹ , M.D. Sokoloff⁶⁶ , F.J.P. Soler⁶⁰ , A. Solomin⁵⁵ <img alt="ORCID iD icon" data-bbox="2421

- A. Solovev⁴⁴ , K. Solovieva²⁰ , N. S. Sommerfeld¹⁸ , R. Song¹ , Y. Song⁵⁰ ,
 Y. Song^{4,d} , Y. S. Song⁶ , F.L. Souza De Almeida⁶⁹ , B. Souza De Paula³ ,
 K.M. Sowa⁴⁰ , E. Spadaro Norella^{29,n} , E. Spedicato²⁵ , J.G. Speer¹⁹ , P. Spradlin⁶⁰ ,
 V. Sriskaran⁴⁹ , F. Stagni⁴⁹ , M. Stahl⁷⁸ , S. Stahl⁴⁹ , S. Stanislaus⁶⁴ , M.
 Stefaniak⁸⁸ , E.N. Stein⁴⁹ , O. Steinkamp⁵¹ , H. Stevens¹⁹ , D. Strekalina⁴⁴ , Y. Su⁷ ,
 F. Suljik⁶⁴ , J. Sun³² , J. Sun⁶³ , L. Sun⁷⁵ , D. Sundfeld² , W. Sutcliffe⁵¹ ,
 V. Svintozelskyi⁴⁸ , K. Swientek⁴⁰ , F. Swystun⁵⁶ , A. Szabelski⁴² , T. Szumlak⁴⁰ ,
 Y. Tan^{4,d} , Y. Tang⁷⁵ , Y. T. Tang⁷ , M.D. Tat²² , J. A. Teijeiro Jimenez⁴⁷ ,
 A. Terentev⁴⁴ , F. Terzuoli^{35,x} , F. Teubert⁴⁹ , E. Thomas⁴⁹ , D.J.D. Thompson⁵⁴ , A.
 R. Thomson-Strong⁵⁹ , H. Tilquin⁶² , V. Tisserand¹¹ , S. T'Jampens¹⁰ , M. Tobin^{5,49} ,
 T. T. Todorov²⁰ , L. Tomassetti^{26,m} , G. Tonani³⁰ , X. Tong⁶ , T. Tork³⁰ ,
 D. Torres Machado² , L. Toscano¹⁹ , D.Y. Tou^{4,d} , C. Trippl⁴⁶ , G. Tuci²² ,
 N. Tuning³⁸ , L.H. Uecker²² , A. Ukleja⁴⁰ , D.J. Unverzagt²² , A. Upadhyay⁴⁹ , B.
 Urbach⁵⁹ , A. Usachov³⁹ , A. Ustyuzhanin⁴⁴ , U. Uwer²² , V. Vagnoni^{25,49} , V.
 Valcarce Cadenas⁴⁷ , G. Valenti²⁵ , N. Valls Canudas⁴⁹ , J. van Eldik⁴⁹ ,
 H. Van Hecke⁶⁸ , E. van Herwijnen⁶² , C.B. Van Hulse^{47,aa} , R. Van Laak⁵⁰ ,
 M. van Veghel³⁸ , G. Vasquez⁵¹ , R. Vazquez Gomez⁴⁵ , P. Vazquez Regueiro⁴⁷ ,
 C. Vázquez Sierra⁸⁴ , S. Vecchi²⁶ , J. Velilla Serna⁴⁸ , J.J. Velthuis⁵⁵ , M. Veltri^{27,y} ,
 A. Venkateswaran⁵⁰ , M. Verdolgla³² , M. Vesterinen⁵⁷ , W. Vetens⁶⁹ , D.
 Vico Benet⁶⁴ , P. Vidrier Villalba⁴⁵ , M. Vieites Diaz^{47,49} , X. Vilasis-Cardona⁴⁶ ,
 E. Vilella Figueras⁶¹ , A. Villa²⁵ , P. Vincent¹⁶ , B. Vivacqua³ , F.C. Volle⁵⁴ ,
 D. vom Bruch¹³ , N. Voropaev⁴⁴ , K. Vos⁸² , C. Vrahas⁵⁹ , J. Wagner¹⁹ , J. Walsh³⁵ ,
 E.J. Walton^{1,57} , G. Wan⁶ , A. Wang⁷ , B. Wang⁵ , C. Wang²² , G. Wang⁸ ,
 H. Wang⁷⁴ , J. Wang⁶ , J. Wang⁵ , J. Wang^{4,d} , J. Wang⁷⁵ , M. Wang⁴⁹ , N. W.
 Wang⁷ , R. Wang⁵⁵ , X. Wang⁸ , X. Wang⁷³ , X. W. Wang⁶² , Y. Wang⁷⁶ ,
 Y. Wang⁶ , Y. H. Wang⁷⁴ , Z. Wang¹⁴ , Z. Wang³⁰ , J.A. Ward⁵⁷ , M. Waterlaat⁴⁹ ,
 N.K. Watson⁵⁴ , D. Websdale⁶² , Y. Wei⁶ , Z. Weida⁷ , J. Wendel⁸⁴ ,
 B.D.C. Westhenry⁵⁵ , C. White⁵⁶ , M. Whitehead⁶⁰ , E. Whiter⁵⁴ ,
 A.R. Wiederhold⁶³ , D. Wiedner¹⁹ , M. A. Wiegertjes³⁸ , C. Wild⁶⁴ ,
 G. Wilkinson^{64,49} , M.K. Wilkinson⁶⁶ , M. Williams⁶⁵ , M. J. Williams⁴⁹ ,
 M.R.J. Williams⁵⁹ , R. Williams⁵⁶ , S. Williams⁵⁵ , Z. Williams⁵⁵ , F.F. Wilson⁵⁸ ,
 M. Winn¹² , W. Wislicki⁴² , M. Witek⁴¹ , L. Witola¹⁹ , T. Wolf²² , E. Wood⁵⁶ ,
 G. Wormser¹⁴ , S.A. Wotton⁵⁶ , H. Wu⁶⁹ , J. Wu⁸ , X. Wu⁷⁵ , Y. Wu^{6,56} , Z. Wu⁷ ,
 K. Wyllie⁴⁹ , S. Xian⁷³ , Z. Xiang⁵ , Y. Xie⁸ , T. X. Xing³⁰ , A. Xu^{35,t} , L. Xu^{4,d} ,
 L. Xu^{4,d} , M. Xu⁴⁹ , Z. Xu⁴⁹ , Z. Xu⁵ , K. Yang⁶² , X. Yang⁶ ,
 Y. Yang¹⁵ , Y. Yang⁷⁹ , Z. Yang⁶ , V. Yeroshenko¹⁴ , H. Yeung⁶³ , H. Yin⁸ , X.
 Yin⁷ , C. Y. Yu⁶ , J. Yu⁷² , X. Yuan⁵ , Y. Yuan^{5,7} , E. Zaffaroni⁵⁰ , J.
 A. Zamora Saa⁷¹ , M. Zavertyaev²¹ , M. Zdybal⁴¹ , F. Zenesini²⁵ , C. Zeng^{5,7} ,
 M. Zeng^{4,d} , C. Zhang⁶ , D. Zhang⁸ , J. Zhang⁷ , L. Zhang^{4,d} , R. Zhang⁸ ,
 S. Zhang⁶⁴ , S. L. Zhang⁷² , Y. Zhang⁶ , Y. Z. Zhang^{4,d} , Z. Zhang^{4,d} , Y. Zhao²² ,
 A. Zhelezov²² , S. Z. Zheng⁶ , X. Z. Zheng^{4,d} , Y. Zheng⁷ , T. Zhou⁶ , X. Zhou⁸ ,
 Y. Zhou⁷ , V. Zhokovska⁵⁷ , L. Z. Zhu⁷ , X. Zhu^{4,d} , X. Zhu⁸ , Y. Zhu¹⁷ ,
 V. Zhukov¹⁷ , J. Zhuo⁴⁸ , Q. Zou^{5,7} , D. Zuliani^{33,r} , G. Zunic²⁸

¹School of Physics and Astronomy, Monash University, Melbourne, Australia

²Centro Brasileiro de Pesquisas Físicas (CBPF), Rio de Janeiro, Brazil

³Universidade Federal do Rio de Janeiro (UFRJ), Rio de Janeiro, Brazil

⁴Department of Engineering Physics, Tsinghua University, Beijing, China

⁵Institute Of High Energy Physics (IHEP), Beijing, China

⁶School of Physics State Key Laboratory of Nuclear Physics and Technology, Peking University, Beijing, China

- ⁷University of Chinese Academy of Sciences, Beijing, China
⁸Institute of Particle Physics, Central China Normal University, Wuhan, Hubei, China
⁹Consejo Nacional de Rectores (CONARE), San Jose, Costa Rica
¹⁰Université Savoie Mont Blanc, CNRS, IN2P3-LAPP, Annecy, France
¹¹Université Clermont Auvergne, CNRS/IN2P3, LPC, Clermont-Ferrand, France
¹²Université Paris-Saclay, Centre d'Etudes de Saclay (CEA), IRFU, Saclay, France, Gif-Sur-Yvette, France
¹³Aix Marseille Univ, CNRS/IN2P3, CPPM, Marseille, France
¹⁴Université Paris-Saclay, CNRS/IN2P3, IJCLab, Orsay, France
¹⁵Laboratoire Leprince-Ringuet, CNRS/IN2P3, Ecole Polytechnique, Institut Polytechnique de Paris, Palaiseau, France
¹⁶Laboratoire de Physique Nucléaire et de Hautes Énergies (LPNHE), Sorbonne Université, CNRS/IN2P3, F-75005 Paris, France, Paris, France
¹⁷I. Physikalisches Institut, RWTH Aachen University, Aachen, Germany
¹⁸Universität Bonn - Helmholtz-Institut für Strahlen und Kernphysik, Bonn, Germany
¹⁹Fakultät Physik, Technische Universität Dortmund, Dortmund, Germany
²⁰Physikalisches Institut, Albert-Ludwigs-Universität Freiburg, Freiburg, Germany
²¹Max-Planck-Institut für Kernphysik (MPIK), Heidelberg, Germany
²²Physikalisches Institut, Ruprecht-Karls-Universität Heidelberg, Heidelberg, Germany
²³School of Physics, University College Dublin, Dublin, Ireland
²⁴INFN Sezione di Bari, Bari, Italy
²⁵INFN Sezione di Bologna, Bologna, Italy
²⁶INFN Sezione di Ferrara, Ferrara, Italy
²⁷INFN Sezione di Firenze, Firenze, Italy
²⁸INFN Laboratori Nazionali di Frascati, Frascati, Italy
²⁹INFN Sezione di Genova, Genova, Italy
³⁰INFN Sezione di Milano, Milano, Italy
³¹INFN Sezione di Milano-Bicocca, Milano, Italy
³²INFN Sezione di Cagliari, Monserrato, Italy
³³INFN Sezione di Padova, Padova, Italy
³⁴INFN Sezione di Perugia, Perugia, Italy
³⁵INFN Sezione di Pisa, Pisa, Italy
³⁶INFN Sezione di Roma La Sapienza, Roma, Italy
³⁷INFN Sezione di Roma Tor Vergata, Roma, Italy
³⁸Nikhef National Institute for Subatomic Physics, Amsterdam, Netherlands
³⁹Nikhef National Institute for Subatomic Physics and VU University Amsterdam, Amsterdam, Netherlands
⁴⁰AGH - University of Krakow, Faculty of Physics and Applied Computer Science, Kraków, Poland
⁴¹Henryk Niewodniczanski Institute of Nuclear Physics Polish Academy of Sciences, Kraków, Poland
⁴²National Center for Nuclear Research (NCBJ), Warsaw, Poland
⁴³Horia Hulubei National Institute of Physics and Nuclear Engineering, Bucharest-Magurele, Romania
⁴⁴Authors affiliated with an institute formerly covered by a cooperation agreement with CERN.
⁴⁵ICCUB, Universitat de Barcelona, Barcelona, Spain
⁴⁶La Salle, Universitat Ramon Llull, Barcelona, Spain
⁴⁷Instituto Galego de Física de Altas Enerxías (IGFAE), Universidade de Santiago de Compostela, Santiago de Compostela, Spain
⁴⁸Instituto de Fisica Corpuscular, Centro Mixto Universidad de Valencia - CSIC, Valencia, Spain
⁴⁹European Organization for Nuclear Research (CERN), Geneva, Switzerland
⁵⁰Institute of Physics, Ecole Polytechnique Fédérale de Lausanne (EPFL), Lausanne, Switzerland
⁵¹Physik-Institut, Universität Zürich, Zürich, Switzerland
⁵²NSC Kharkiv Institute of Physics and Technology (NSC KIPT), Kharkiv, Ukraine
⁵³Institute for Nuclear Research of the National Academy of Sciences (KINR), Kyiv, Ukraine
⁵⁴School of Physics and Astronomy, University of Birmingham, Birmingham, United Kingdom
⁵⁵H.H. Wills Physics Laboratory, University of Bristol, Bristol, United Kingdom
⁵⁶Cavendish Laboratory, University of Cambridge, Cambridge, United Kingdom
⁵⁷Department of Physics, University of Warwick, Coventry, United Kingdom

- ⁵⁸STFC Rutherford Appleton Laboratory, Didcot, United Kingdom
⁵⁹School of Physics and Astronomy, University of Edinburgh, Edinburgh, United Kingdom
⁶⁰School of Physics and Astronomy, University of Glasgow, Glasgow, United Kingdom
⁶¹Oliver Lodge Laboratory, University of Liverpool, Liverpool, United Kingdom
⁶²Imperial College London, London, United Kingdom
⁶³Department of Physics and Astronomy, University of Manchester, Manchester, United Kingdom
⁶⁴Department of Physics, University of Oxford, Oxford, United Kingdom
⁶⁵Massachusetts Institute of Technology, Cambridge, MA, United States
⁶⁶University of Cincinnati, Cincinnati, OH, United States
⁶⁷University of Maryland, College Park, MD, United States
⁶⁸Los Alamos National Laboratory (LANL), Los Alamos, NM, United States
⁶⁹Syracuse University, Syracuse, NY, United States
⁷⁰Pontifícia Universidade Católica do Rio de Janeiro (PUC-Rio), Rio de Janeiro, Brazil, associated to ³
⁷¹Universidad Andres Bello, Santiago, Chile, associated to ⁵¹
⁷²School of Physics and Electronics, Hunan University, Changsha City, China, associated to ⁸
⁷³Guangdong Provincial Key Laboratory of Nuclear Science, Guangdong-Hong Kong Joint Laboratory of Quantum Matter, Institute of Quantum Matter, South China Normal University, Guangzhou, China, associated to ⁴
⁷⁴Lanzhou University, Lanzhou, China, associated to ⁵
⁷⁵School of Physics and Technology, Wuhan University, Wuhan, China, associated to ⁴
⁷⁶Henan Normal University, Xinxiang, China, associated to ⁸
⁷⁷Departamento de Fisica , Universidad Nacional de Colombia, Bogota, Colombia, associated to ¹⁶
⁷⁸Ruhr Universitaet Bochum, Fakultaet f. Physik und Astronomie, Bochum, Germany, associated to ¹⁹
⁷⁹Eotvos Lorand University, Budapest, Hungary, associated to ⁴⁹
⁸⁰Faculty of Physics, Vilnius University, Vilnius, Lithuania, associated to ²⁰
⁸¹Van Swinderen Institute, University of Groningen, Groningen, Netherlands, associated to ³⁸
⁸²Universiteit Maastricht, Maastricht, Netherlands, associated to ³⁸
⁸³Tadeusz Kosciuszko Cracow University of Technology, Cracow, Poland, associated to ⁴¹
⁸⁴Universidade da Coruña, A Coruña, Spain, associated to ⁴⁶
⁸⁵Department of Physics and Astronomy, Uppsala University, Uppsala, Sweden, associated to ⁶⁰
⁸⁶Taras Shevchenko University of Kyiv, Faculty of Physics, Kyiv, Ukraine, associated to ¹⁴
⁸⁷University of Michigan, Ann Arbor, MI, United States, associated to ⁶⁹
⁸⁸Ohio State University, Columbus, United States, associated to ⁶⁸

^aUniversidade Estadual de Campinas (UNICAMP), Campinas, Brazil

^bCentro Federal de Educacão Tecnológica Celso Suckow da Fonseca, Rio De Janeiro, Brazil

^cDepartment of Physics and Astronomy, University of Victoria, Victoria, Canada

^dCenter for High Energy Physics, Tsinghua University, Beijing, China

^eHangzhou Institute for Advanced Study, UCAS, Hangzhou, China

^fLIP6, Sorbonne Université, Paris, France

^gLamarr Institute for Machine Learning and Artificial Intelligence, Dortmund, Germany

^hUniversidad Nacional Autónoma de Honduras, Tegucigalpa, Honduras

ⁱUniversità di Bari, Bari, Italy

^jUniversità di Bergamo, Bergamo, Italy

^kUniversità di Bologna, Bologna, Italy

^lUniversità di Cagliari, Cagliari, Italy

^mUniversità di Ferrara, Ferrara, Italy

ⁿUniversità di Genova, Genova, Italy

^oUniversità degli Studi di Milano, Milano, Italy

^pUniversità degli Studi di Milano-Bicocca, Milano, Italy

^qUniversità di Modena e Reggio Emilia, Modena, Italy

^rUniversità di Padova, Padova, Italy

^sUniversità di Perugia, Perugia, Italy

^tScuola Normale Superiore, Pisa, Italy

^uUniversità di Pisa, Pisa, Italy

^vUniversità della Basilicata, Potenza, Italy

^wUniversità di Roma Tor Vergata, Roma, Italy

^x Università di Siena, Siena, Italy

^y Università di Urbino, Urbino, Italy

^z Universidad de Ingeniería y Tecnología (UTEC), Lima, Peru

^{aa} Universidad de Alcalá, Alcalá de Henares , Spain

[†]Deceased